1964

Flow instability in a naturally circulating boiling water reactor

Mark Arthur McDermott
Iowa State University

FLOW INSTABILITY IN A NATURALLY CIRCULATING BOILING WATER REACTOR

by

Mark Arthur McDermott

A Dissertation Submitted to the
Graduate Faculty in Partial Fulfillment of
The Requirements for the Degree of
DOCTOR OF PHILOSOPHY

Major Subject: Nuclear Engineering

Approved:

Signature was redacted for privacy.
In Charge of Major Work

Signature was redacted for privacy.
Head of Major Department

Signature was redacted for privacy.
Dean of Graduate College

Iowa State University
Of Science and Technology
Ames, Iowa

1964

TABLE OF CONTENTS

I. INTRODUCTION

The rate at which useful energy can be obtained from a nuclear reactor is usually limited by the ability of the heat removal system to remove energy from the reactor core. The reactor coolant must keep the fuel elements below their maximum permissible operating temperatures and also transport the newly released energy, in the form of heat, out of the core to where it can be converted into other useful forms of energy. The ideal reactor coolant system would keep the reactor at a desired temperature and still be capable of removing any desired amount of heat.

The reactor coolant, in addition to its heat removal role, often serves as a moderator for the reactor. Changes in temperature and density of the coolant thus affect the reactivity, and hence, the control of a nuclear reactor.

The use of boiling water as a reactor coolant has many of the desired characteristics of an ideal coolant. Large quantities of heat can be removed per pound of coolant due to the latent heat associated with the phase change, and the temperature of the coolant remains nearly constant once boiling has begun. Another advantage of boiling water as a reactor coolant is that the steam produced can be used directly in steam turbine generators without additional heat exchangers or steam drums. . The heat removal rate in a boiling water reactor is usually limited by the rate at which the

coolant can be circulated through the reactor.

The apparent advantages of a boiling water reactor have usually been measured against one disadvantage--lack of stability. The feedback between reactivity and boiling voids makes such a reactor appear very unstable. It is interesting to note that in the late 1940's when a boiling water reactor was first considered in the United States it was thought that this type of reactor would have a poor chance of feasibility (17). It was considered highly unlikely that such a reactor would be stable. Much of the preliminary experimental work performed before the first boiling water reactor was designed and built was directed towards determining how rapidly heat could be removed from a reactor fuel channel by a boiling liquid, and determining whether or not the flow of the boiling coolant remained stable.

The BORAX I reactor, which operated at atmospheric pressure, demonstrated in 1953 that a boiling water reactor could operate safely and that boiling water reactors may have a high degree of stability. Other experiments (42, 17) indicated that a boiling water reactor was inherently stable, and yet under certain fixed operating conditions flow and power oscillations occurred. These oscillations were large and repeated, and in some cases divergent. In their more violent form they could seriously limit the usefulness of a boiling water reactor as a source of power.

A boiling water reactor is a complex system. Its gross behavior is a combination of interrelated and simultaneous feedback among nuclear characteristics, heat transfer characteristics, and hydraulic characteristics, occurring in a complex geometric array. The detailed interaction of such a system is difficult to analyze. There is considerable evidence (3) that the single most important cause of power oscillations in a boiling water reactor is from hydrodynamic processes. Nuclear characteristics may cause feedback and amplification once an oscillation has started but the triggering device is frequently hydrodynamic, or the oscillations may be hydrodynamic only.

Electrically heated boiling water loops have been used to predict the behavior of a naturally circulating boiling water reactor (42, 71). Such loops do not have the complex interrelation between power and hydraulic characteristics that a nuclear reactor has, but they are used to predict when hydrodynamic instability will occur. An understanding of the oscillatory behavior of a boiling water loop is the first step towards understanding the more complex oscillatory behavior of a boiling water reactor.

This investigation describes a method for predicting instabilities in a boiling water loop which has two parallel risers with heat generation which are connected to a downcomer with no heat generation. The additional riser leg introduces

an interaction that is not present in a simple boiling loop and permits forms of oscillations that can not occur in a naturally circulating loop with a single riser.

II. TWO-PHASE FLOW

A knowledge of the parameters and mechanics of two-phase flow is necessary before trying to analyze the causes of instabilities in boiling systems. Two-phase flow occurs when a liquid and a vapor are being simultaneously transmitted in a closed channel.

Two-phase flow usually occurs in one of the following forms:

a. Liquid and vapor are stratified. This type of flow can occur when a liquid and a vapor are transmitted at low velocities in a horizontal pipe.

b. The liquid carries the gas in bubble form. This type of flow occurs in most naturally circulating boiling systems.

c. The vapor carries the liquid in droplet form and there is sufficient liquid present to wet the walls of the channel. This type of flow is commonly known as fog flow.

d. The vapor and liquid are transmitted in alternate phases. This type of flow is commonly known as slug flow.

The flow pattern may not be sharply defined. In vertical flow, for example, the bubbles may coalesce in the center of the channel and the resulting flow becomes a form of stratified flow known as core flow.

The flow can be further catagorized as to whether the flow in each phase is turbulent or viscous. In boiling water

reactors the two-phase flow is normally of type b described above. This study will be limited to this type of flow.

One of the most difficult parameters to determine in two-phase flow is the relation between the liquid velocity, V, and the vapor velocity, V". In the literature these are usually expressed by the slip ratis, $V''/_V$, or the slip velocity, V"-V.

When a liquid and a vapor are both rising in a channel and the liquid carries the vapor in bubble form the relative velocity of the bubble to the liquid is upward. The velocity of the liquid at the channel walls is zero, and the maximum liquid velocity occurs away from the channel walls. The result is that the bubbles are accelerated away from the channel walls by Bernoulli forces. Thus, in vertical, or counter-gravity flow, the bubbles are concentrated away from the walls and in the region of maximum liquid velocity. The resulting average relative velocity and the average slip velocity in the channel are not the relative velocity and the slip velocity of a single bubble to its surrounding liquid, but are actually larger due to the increased velocity of the liquid in the center of the channel where most of the bubbles are concentrated. Sufficient concentration of bubbles in the center of a channel results in coalescence of the bubbles, and this coalescence can result in core flow in which the center of a channel is occupied by vapor and the liquid occupies the outer regions.

This results in a further augmentation of the average relative velocity.

When the liquid and vapor are flowing downward in a channel the Bernoulli forces tend to move the bubbles toward the center of the channel, but Magnus forces (13) tend to move the bubbles away from the center, and the resultant flow distribution, in a circular channel, is a flow where the bubbles are concentrated in an annulus. At larger downward velocities the Bernoulli forces predominate the core flow results.

Two other important two-phase flow parameters are the vapor fraction, $\emptyset$, and the quality, x. The vapor fraction is the ratio of the cross sectional area of a channel occupied by vapor to the total area of the channel. The quality is the ratio of the mass flow rate of vapor to the total mass flow rate.

The void fraction, quality, and slip ratio are related by the following equations, where all values are average values:

$$x = \frac{1}{1 + \frac{V}{V''}\ \frac{\rho}{\rho''}\ \frac{1-\emptyset}{\emptyset}} \qquad 1$$

$$\emptyset = \frac{1}{1 + \frac{\rho''}{\rho}\ \frac{V''}{V}\ \frac{1-x}{x}} \qquad 2$$

$$\frac{V''}{V} = \frac{\rho}{\rho''}\ \frac{1-\emptyset}{\emptyset}\ \frac{x}{1-x} \qquad 3$$

Similar equations may be derived relating voids, quality,

and the relative velocity.

Other equations which need to be reviewed to better understand the literature are the conservation of mass, momentum, and energy equations for two-phase flow. For one dimensional flow these respective equations are as follows.

$$\frac{\partial}{\partial x}(V''\rho''\emptyset + V\rho(1-\emptyset)) + \frac{\partial}{\partial t}(\rho(1-\emptyset) + \rho''\emptyset) = 0 \qquad 4$$

$$dF_x = \frac{d}{dt} \quad (\rho V(1-\emptyset) + \rho''V''\emptyset) \qquad 5$$

$$\frac{\partial}{\partial x}(h_v V''\rho''\emptyset + h_f V\rho(1-\emptyset) - \frac{Q}{g} + \frac{\partial}{\partial t}(\rho(1-\emptyset)h_f + \rho''\emptyset h_v) = 0 \qquad 6$$

In equation 5 dF_x represents the resultant of all the forces acting on the differential element. These forces would normally be due to friction, pressure, and gravity. In equation 6 Q represents the rate at which heat is being added per unit volume. The kinetic energy and elevation terms have been dropped in this equation because at practical reactor circulation velocities the kinetic energy and elevation energy of the fluid are negligible in comparison to the internal or heat energy stored in the fluid.

III. LITERATURE REVIEW

The concept and successful operation of a boiling water reactor provided the impetus for dozens of investigations into two-phase flow. Some work had been conducted prior to the advent of the boiling water reactor, but the bulk of the investigations have been conducted during the past decade.

The literature review is divided into two sections. The first section describes works done to relate the parameters that are associated with two-phase flow and the prediction of steady state two-phase flow conditions. These must be known before any instability equations can be solved. The second section describes experimental and theoretical works associated with the phenomena of instability in two-phase flow.

A. Two-Phase Flow Literature Review

Some of the earlier investigations were directed towards determining the relative motion of bubbles in a two-phase mixture and in determining the friction losses associated with two-phase flow. One of the earliest attempts to determine the bubble velocities is that of Behringer (11) who in 1934 measured the voids and velocity when steam was bubbled through a stationary column of water. His results were presented in the forms of curves and no expression was derived which would predict the velocity of the rising bubbles.

Another important pre-nuclear investigation is the

Martinelli and Nelson correlation of two-phase friction losses and single-phase friction losses (52). Martinelli predicted the two-phase friction loss as a function of the single-phase friction loss through a dimensionless parameter involving the liquid and vapor densities, viscosities, and flow rates. His work relates the momentum exchange between the two phases to the friction loss of the two-phase mixture and he arrives at a series of plots for different flow regimes. Lockhart and Martinelli (46) predicted the slip velocity from a similar analysis. These prediction equations do not agree as well with experimental data as some later investigations, but this work remains as one of the better-known papers in the field.

In the United States most of the investigations necessary to design the first boiling water reactors were conducted at Argonne National Laboratory, and a concise review of much of the work done there prior to 1958 was presented by Lottes at Geneva in 1958 (49). In this paper a method for predicting circulation rates in a naturally circulating boiling reactor is outlined. Curves are presented which show the slip ratio as a function of pressure and inlet velocity and a general method is presented for calculating the steady state circulation rate of a boiling water reactor. The method presented provides a quickly converging trial and error solution using the experimental curves to determine the steady state flow

rates.

Bankoff (5) has determined steady-state values for the slip ratio by assuming the velocity and the void fraction obey a power law distribution in the radial direction, and that the local bubble slip velocity is constant. He then derives expressions for the void fraction and average slip ratio in terms of the exponents in the distribution. These are lumped in a parameter K which is a slowly varying quantity for all reasonable velocity and void fraction profiles. The equation he obtains for slip ratio is

$$\frac{V''}{V} = \frac{1-\emptyset}{K-\emptyset} \qquad 7$$

Where K is a slowly varying parameter having values of 0.70 to 0.95 for reasonable flow velocities. Bankoff's equation for shear stress compares favorably with that of Martinelli and Nelson.

Levy (45) developed a theoretical equation for the quality and frictional loss by assuming a model in which momentum is conserved between the vapor and the liquid every time the quality, void fraction and velocity change. This exchange of momentum tends to maintain the equality of frictional and head losses of the two phases. This is similar to the model used by Martinelli and Nelson in their analysis. This theory gives good prediction of pressure drops in two-phase flow, but is not quite as successful in predicting void fractions. Levy's theory predicts that the ratio of friction

loss in two-phase flow to friction loss in liquid flow only is given by $1/(1-\emptyset^2)$ and the slip ratio is nearly equal to

$$\frac{V''}{V} = \sqrt{\frac{\rho}{\rho''} \cdot 2\emptyset} \qquad 8$$

Foglia (24) gives a good comparison of the equations of Bankoff, Levy, and the working curves of Argonne National Laboratory. He also presents an empirical equation for predicting voids in regions of subcooled boiling.

Wilson (66) has determined an empirical equation for the velocity of steam bubbles in a bubbling two-phase mixture. His data have been reduced to a dimensionless equation

$$\phi = A\left(\frac{\rho}{\rho - \rho''}\right)^{0.32}\left(\frac{\sqrt{\frac{\sigma}{g(\rho-\rho'')}}}{d}\right)^{0.19}\left[\frac{V''}{\left(g\sqrt{\frac{\sigma}{g(\rho-\rho'')}}\right)^{1/2}}\right]^{n} \qquad 9$$

where $n = 1.78$ and $A = 0.136$ when $\dfrac{V''}{\left(g\sqrt{\frac{\sigma}{g(\rho-\rho'')}}\right)^{1/2}} < 5$

and $n = 0.78$ and $A = 0.75$ when $\dfrac{V''}{\left(g\sqrt{\frac{\sigma}{g(\rho-\rho'')}}\right)^{1/2}} > 5$

The d in equation 9 represents the diameter of the channel. The data were taken in two, four, and nineteen inch diameter vessels, and it is seen that the bubble velocity is somewhat dependent upon the diameter of the vessel.

One of the more important foreign contributions to the investigation of two-phase flow is that of Kholodovskiy (36). Kholodovskiy has correlated two-phase flow data from steam boiler circulation and unheated pipes and arrived at a dimensionless plot and prediction equation which describes the flow of the components inside boiler tubes. Kholodovskiy chose to describe the flow in different parameters than those used by most American investigators. Velocities are described in terms of the reduced velocity, which is the velocity one phase would have if it proceeded along the entire cross section of the channel. The reduced velocity of the liquid, U, is then $V(1-\emptyset)$ and the reduced velocity of the vapor, U", is $V''\emptyset$. The velocity of the mixture, W, is the sum of U and U". Kholodovskiy's principal reason for selecting these parameters was his success in correlating the two-phase flow data of other scientists when these data were analyzed using these parameters. Experimental data correlating steam-water, steam-mercury, and air-water are reduced to an equation of the form

$$\frac{V''\mu K}{\sigma} = a\left(\frac{W\mu}{\sigma} K\right)^n \qquad 10$$

where K is $\frac{g\mu^2}{\sigma^3\rho}$ and a and n are experimentally determined constants.

Thus for a given pressure in a steam-water system,

equation 10 reduces to the form

$$V'' = cW^n \qquad 10\text{-a}$$

where $c = a\left(\frac{\mu K}{\sigma}\right)^{n-1}$. Since $\emptyset = \frac{U''}{V''}$ it follows that

$$\emptyset = \frac{U''}{cW^n} \qquad 11$$

Figure 1 shows a plot of the generalized function determined by Kholodovskiy. For the right portion of the curve (the solid straight line) n = 0.981 and a = 0.647, and for the left portion of the curve, or where log $(W\mu/\sigma K) < -15$, a = 0.0525, and n = 0.84.

Kholodovskiy's analysis showed that the relation between voids and vapor velocity was independent of channel size. However, the data he analyzed were obtained from pipes having diameters of 23 to 76 millimeters. His analysis further indicated that the regularity of the movement of gas-liquid mixtures in vertical pipes is not altered by a variation in the pressure or gas content of the mixture within wide limits.

An extensive experimental program carried out at Cambridge University (30) adds considerable data relating friction losses and two-phase flow relations in 1-inch and in 1½-inch bore pipes. No generalized function is presented relating the two-phase flow parameters, but the data are correlated with Kholodovskiy's equations and the correlation is good.

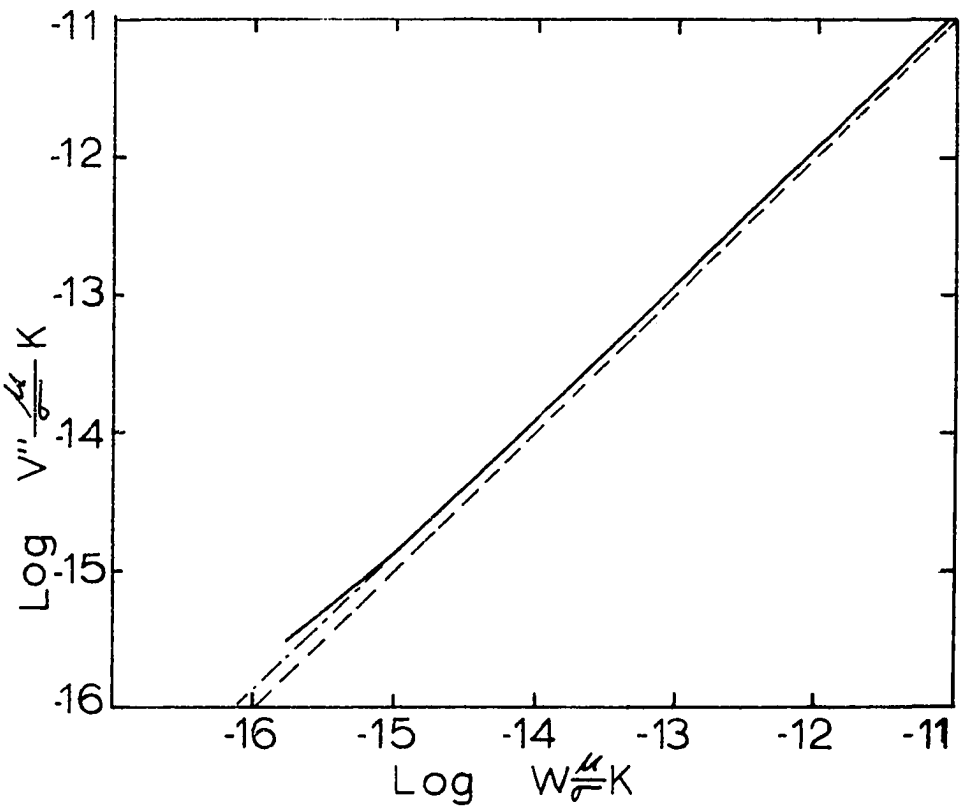

Figure 1. Generalized experimental equation of Kholodovskiy

Considerable insight was gained towards a better understanding of two-phase friction factors as a result of the experimental program at Cambridge. The results were well summarized by Professor D.B. Spalding in the discussion of the paper. He concluded that "one of the most important things to be learned as a result of the work of the authors was that the whole process was very simple! The remarkable fact, which could scarcely have been guessed beforehand, was that the two-phase flow behaved very much like a single-phase one, and that the friction factor was almost constant."

The conclusion drawn by Spalding was verified by Kutateladze (43).

Other general references relating steady-state two-phase flow and two-phase flow friction factors are (26), (32), (39), and (51).

B. Hydraulic Instability Literature Review

Numerous experiments have been conducted and many theories advanced which describe the behavior of oscillatory two-phase flow. A bibliography on this and related subjects has been prepared by Johnson (33). A review of some of the more important contributions prior to 1960 is prepared by Anderson and Lottes (3).

Most investigators, although using various assumptions and models, have started with the basic equations of mass, energy, and momentum for the model and have introduced a fourth

equation which describes the interaction between the two phases.

One of the earliest and most widely known theories for the cause of unstable behavior due to a single phenomenon was the pressure drop-flow rate curve shown in Figure 2. Ledinegg (44) published a paper using this approach in 1938, and this type of instability is frequently known as Ledinegg Instability. In this type of instability it is assumed that a decreasing pressure drop occurs with increasing flow at a point, and that instabilities occur when this point is reached. Beckjord and Levy (10) and Quandt (59) indicate that this is not sufficient cause for oscillation. They reason that a system that is operating at point B will accelerate to point A or point C but that it will not oscillate.

Blubaugh (14) and Quandt (59) have shown that instabilities are caused by many interrelated variables, and that the onset of instability can not be predicted by a single phenomenon as suggested by Ledinegg.

1. Reactor stability experiments

Numerous experiments have been carried out with boiling water reactors at atmospheric pressure and at elevated pressures to determine their stability. These tests are usually of two distinct types--where reactivity is increased in a ramp or step function and reactivity response is recorded, and where reactivity is harmonically oscillated and the resultant

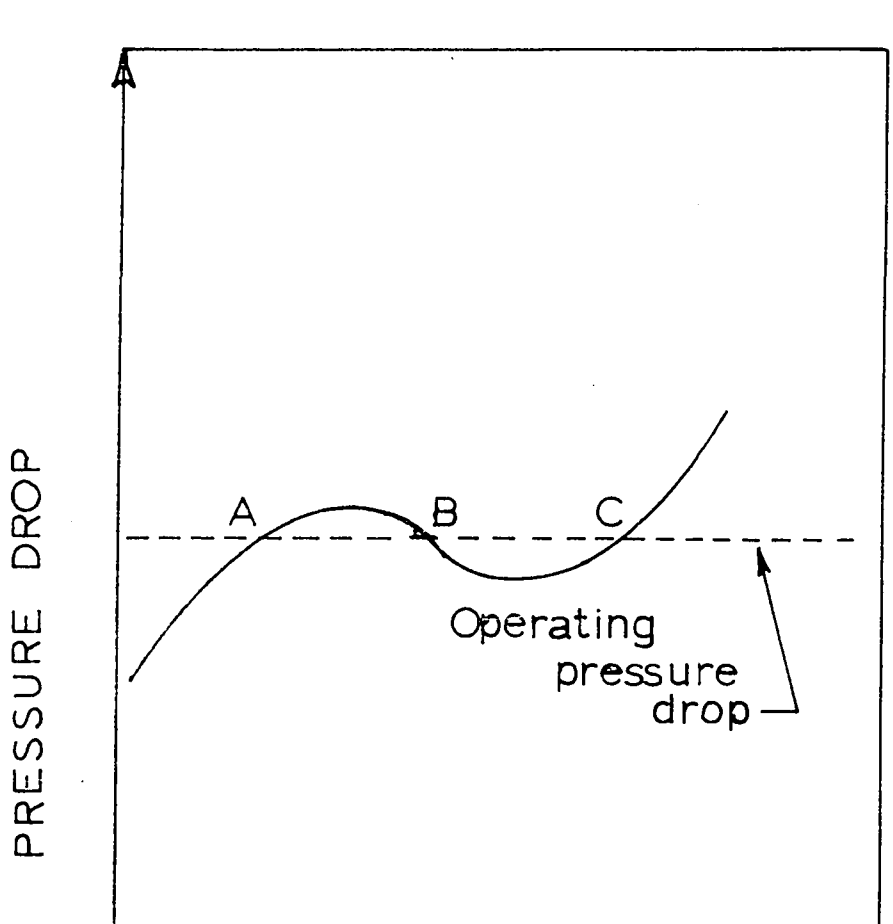

Figure 2. Unstable but non-oscillatory flow condition

harmonic power oscillation observed.

The BORAX and SPERT tests were parametric studies to arrive at design parameters and determine whether or not power oscillations occurred in boiling water reactors. The early BORAX and SPERT tests were limited to step and ramp reactivity inputs, and to operations at steady state. These tests indicated the general stability of boiling water reactors, but also showed that power oscillations did occur, even at steady-state operation, and that these oscillations, were, in some cases, divergent. Descriptions of the tests in BORAX and SPERT tests may be found in references (42), (21), and (70).

Tests using harmonically oscillated reactivity input have been performed on EBWR, Valecitos Boiling Water Reactor, and on BORAX IV (3).

The analysis of forced oscillations of boiling water reactors has in general followed a transfer function approach. In this method of analysis it is necessary to linearize the differential equations which describe the reactor. This limits the validity of results to small variations at fixed operating points.

Beckjord (6) was one of the first to analyze flow variations with transfer functions. He considered the effects of heat transfer, steam voids, steam flashing, and boiling boundary change. He assumed constant slip ratios for steam.

Others who have investigated the feedback transfer function of boiling water reactors include De Shong and Lipinski (20), and Thie (63), and Zivi (70, 71). Zivi points out that the dominant cause of hydrodynamic instability in a boiling water reactor is unstable linear feedback between flow and steam void volume. The power-void transfer function is also dominated by this flow-void feedback, so that both the reactivity feedback type of boiling water reactor instability and the power oscillations arising from hydrodynamic instability have the same cause.

2. Test loop stability experiments

Experimental studies to determine the operating characteristics of naturally circulating electrically heated boiling test loops have been, and are currently being, conducted at various research centers. The general nature of these tests is to determine steady-state circulation rates and to determine the onset of instabilities and the parameters affecting the onset of instabilities.

The test loop at the University of Minnesota is a single loop in which the steam condenses while flowing as a two-phase mixture in the crossover. The onset of instabilities has not been studied, but detailed analyses have been made of the loop while it was oscillating. Wissler (67,68), Garlid, Amundson, and Isbin (27), and George (28) have analyzed the flow of this loop using analog and digital computers. The flow in the loop

exhibited a long period (50-200 sec.) with steady amplitude and non-symmetrical shape.

Wissler combined the conservation equations into finite difference form and programed the equations for a digital computer but the program did not converge. George's model utilized the same data as Wissler, but he made several simplifying assumptions, and his solutions agreed very well with the experimental data.

Garlid, Isbin, and Amundson obtained solutions describing the behavior of test loops by using both analog and digital computers. The analog solutions were not completely satisfactory. The digital computer solution predicted transient behavior very satisfactorily for the Minnesota low-pressure loop. Experimentally determined friction data and flow characteristics were used in analyzing the Minnesota loop.

The model used by Garlid et al. was not as satisfactory in predicting the results of a 300-psi open loop at Argonne. Closed unstable regions rather than limits were predicted, and the prediction of stability in terms of a simgle parameter was found to be impossible. The slip ratio and the nature of its variations were found to be critical in determining the loop behavior. In the low pressure loop constant values of four or five for the slip ratio gave good results.

Electrically heated test loops have been operated at Argonne National Laboratory at pressures up to 600-psi

(51, 42). Open loops were used in which steam was removed from the system and makeup water was added. The primary objective of the experiments was to determine conditions accompanying the onset of oscillations. It was found that the maximum stable power level increased with increasing pressure, was affected by the geometry, and was relatively insensitive to the level of liquid above the riser section. The period of the oscillations observed did not vary greatly and was approximately of one second.

Anderson et al. (2) used an analog computer system similar to Garlid's to solve the time dependent behavior of the two-phase natural circulation systems during transients. The behavior of the model was found to be sensitive to the slip ratio used.

The General Electric Atomic Power Equipment Department has conducted experiments using an electrically heated core in a test loop operating at 1000 psia (8, 10). Instability could not be correlated as a function of any single parameter. The period of oscillation was between 2 and 4 seconds. It was observed that increased subcooling resulted in greater instability.

The Westinghouse Atomic Power Division has conducted tests on an electrically heated 1000 to 1600 psia loop (14). This was a forced circulation loop and the test section was in parallel with a large unheated riser which had the effect of keeping the pressure drop across the heated section constant.

The experimental data showed that the exit steam quality at which oscillations occur is principally a function of pressure and inlet coolant temperature. Periods in the order of one second were observed. A perturbation analysis which was solved on a digital computer was used to predict the coolant conditions at which unstable oscillations begin. The experimental program and analysis were in general agreement.

Space Technology Laboratories operates a test loop with geometry similar to the SPERT reactor. They are conducting tests to determine boiling channel transfer functions (70) and use these to analyze the SPERT instabilities. Their experimental work shows periods of about 0.8 seconds.

A digital computer program for examining hydraulic stability of a single boiling channel in parallel with many other channels has been written by Jones and Dight (34, 35). This program divides the channel into a number of nodes and solves for the instabilities by use of transfer functions. Slip ratios are based on Bankoff's equation and it is assumed that all equations can be linearized. The Nyquist criterion is used to determine whether the system is stable or not. The program also accounts for subcooled boiling and predicts friction multipliers from Martinelli and Nelson two-phase multipliers. One comparison is made with a known system with excellent results.

Beckjord is the author of several papers (6, 7, 8, 10) on

dynamic analysis of natural circulating loops. He uses Lagrangian co-ordinates and perturbs the steady-state system to determine whether or not stability exists.

Beckjord and Harker (9) have collaborated on a computer program (HERCULES) which has been successful in analyzing two-phase flow. This program is for steady-state values and slip ratios are determined from Levy's momentum model.

Other digital computer programs for analyzing two-phase flow include Blubaugh and Quandt (14) who analyze flow through a single channel and with constant pressure drop; Fleck (22), who assumes a constant slip ratio and essentially considers the boiling core as one lumped region; Miller and Pyle (56), who have written a two dimensional program to analyze flow in rectangular fuel elements; and Noyes et al. (57), whose program calculates steady-state two-phase flow parameters in non-dimensional terms.

Other references which were enlightening in analyzing numerical instabilities in finite difference methods with digital computers are works by Longly (47) and Richtmeyer (61).

IV. OBJECT OF RESEARCH

The object of this research is to develop a mathematical model to assist in the prediction of the time dependent behavior of the two-phase flow in each of two parallel risers in a naturally circulating boiling loop. Figure 3 is a schematic representation of the model analyzed.

The additional riser, which is not found in any of the loops previously analyzed, adds a degree of freedom to the system and permits forms of oscillations not found in loops with only one riser such as those examined at Argonne National Laboratory or General Electric. The additional riser also permits a variation in pressure drop across a channel that is not possible in loops such as those analyzed by Quandt (59), where the pressure across the boiling riser was kept constant.

The additional riser makes the loop hydraulically similar to a boiling water reactor containing two distinct heat generation rates. These two distinct heat generation rates could occur from such things as

1. The shadowing effect of a control rod greatly reducing the heat generation rate in adjacent fuel elements.
2. Differences in fuel loading or fuel enrichment in different regions of the reactor core.
3. Regions of low neutron flux, such as the peripheral fuel elements.

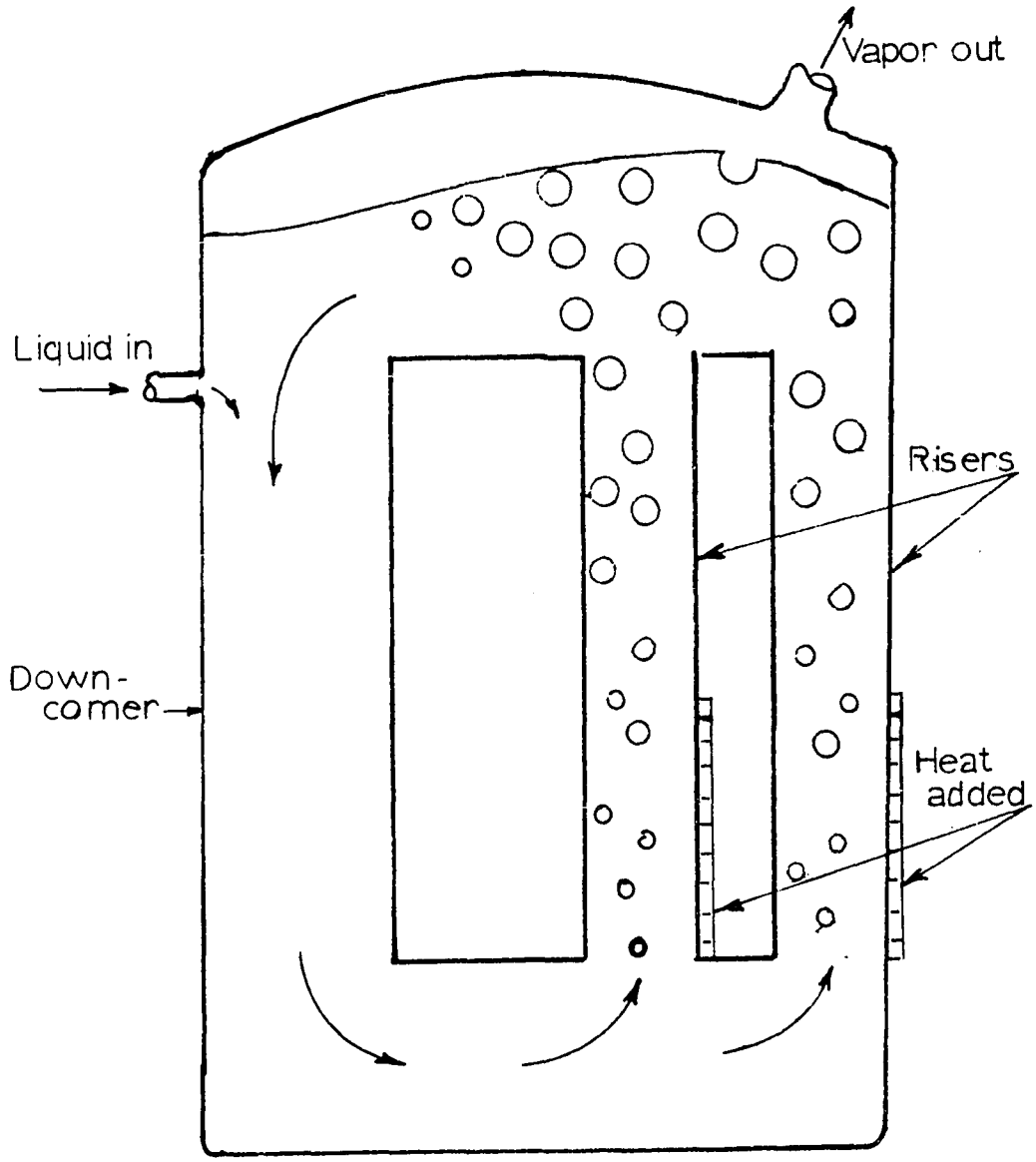

Figure 3.
Natural circulation loop
with parallel risers

4. Regions such as a reflector where the coolant is used primarily as a moderator with little heat generation.

The model shown in Figure 3 will permit flow reversals in one of the risers if the heat production in that channel is sufficiently reduced. This flow reversal is not possible in any of the loop analyses reported in the literature. The possibility of a flow reversal requires that the relation between the liquid and vapor velocities must encompass a wide range of flow conditions and therefore this relation cannot be linearized around an expected operating condition. This means that the assumption of nearly constant slip ratios that many observers have used must be improved and an equation, or series of equations be determined which adequately describes the relation between the two phases for both forward and reversed flow.

The calculation procedure developed in this thesis could be extended to a greater number of risers. This could, for example, be extended to include the prediction of the flow through each fuel channel in a boiling water reactor. The model does not include any void reactivity feedback to the heat generation rate as would be found in a boiling water reactor. Only the hydraulic characteristics of the system are considered. This could, of course, serve as a triggering device for power oscillations, but the system examined involves only hydrodynamic characteristics.

V. DEVELOPMENT OF THE MODEL

In this section the general equations describing the two-phase flow in the model are developed. This development of the model is divided into two sections, the first describing the dynamic relation between the two phases, and the second developing the general differential equations which describe two-phase flow.

A. Two-Phase Flow Relation

Two-phase flow is not completely described unless a relation between the movement of the two phases is known. The hydraulic oscillations examined in this paper include those occurring at low heat generation rates that could result in possible flow reversals. It is therefore necessary to adequately describe the motion between the two phases over a very wide range of flow conditions.

The apparent success of Kholodovskiy in predicting the two-phase flow in vertical risers suggests the use of his model where the fluid is flowing upward. The relation of Kholodovskiy's equation at 600 psi is plotted in Figure 4. Also plotted on the same curve is the equation predicted by Wilson for bubbles moving through a stationary liquid and experimental data from Argonne. (The experimental data do not represent actual data points but are calculated from suggested working curves for slip ratio suggested by Lottes (51). These curves are from experimental data.) Wilson's data were

obtained using zero liquid velocity. This would be a special case of Kholodovskiy's equation where U is equal to zero. It is noted that both Wilson's and Kholodovskiy's equations approach zero as the value of W goes to zero and this can not be the physical case. This would imply a single bubble remains stationary when placed in a stationary liquid. This means that some other model must be used to describe the flow in the regions of low liquid velocity and voids.

To evaluate the bubble velocity as the value of W approaches zero it is assumed that the value of the bubble velocity, V", would be that of a single bubble rising in a stationary liquid when W is equal to zero. The relation between the variables as W approaches zero does not predict the velocity of a single bubble on either of the curves shown on Figure 4. Therefore, an empirical curve fitting the data of the two equations and forced to pass through the desired bubble velocity at zero velocity of the mixture is drawn. This value is obtained from the equation recommended by Zuber (72). For 600 psi this value is 0.51 feet per second.

It should be noted that W can be equal to zero under two different conditions. In the first condition, U and U" are both equal to zero, and in the second condition, U and U" have different algebraic sign and their net sum is equal to zero. In a naturally circulating two-phase mixture the latter condition would be expected to occur only when the liquid velocity

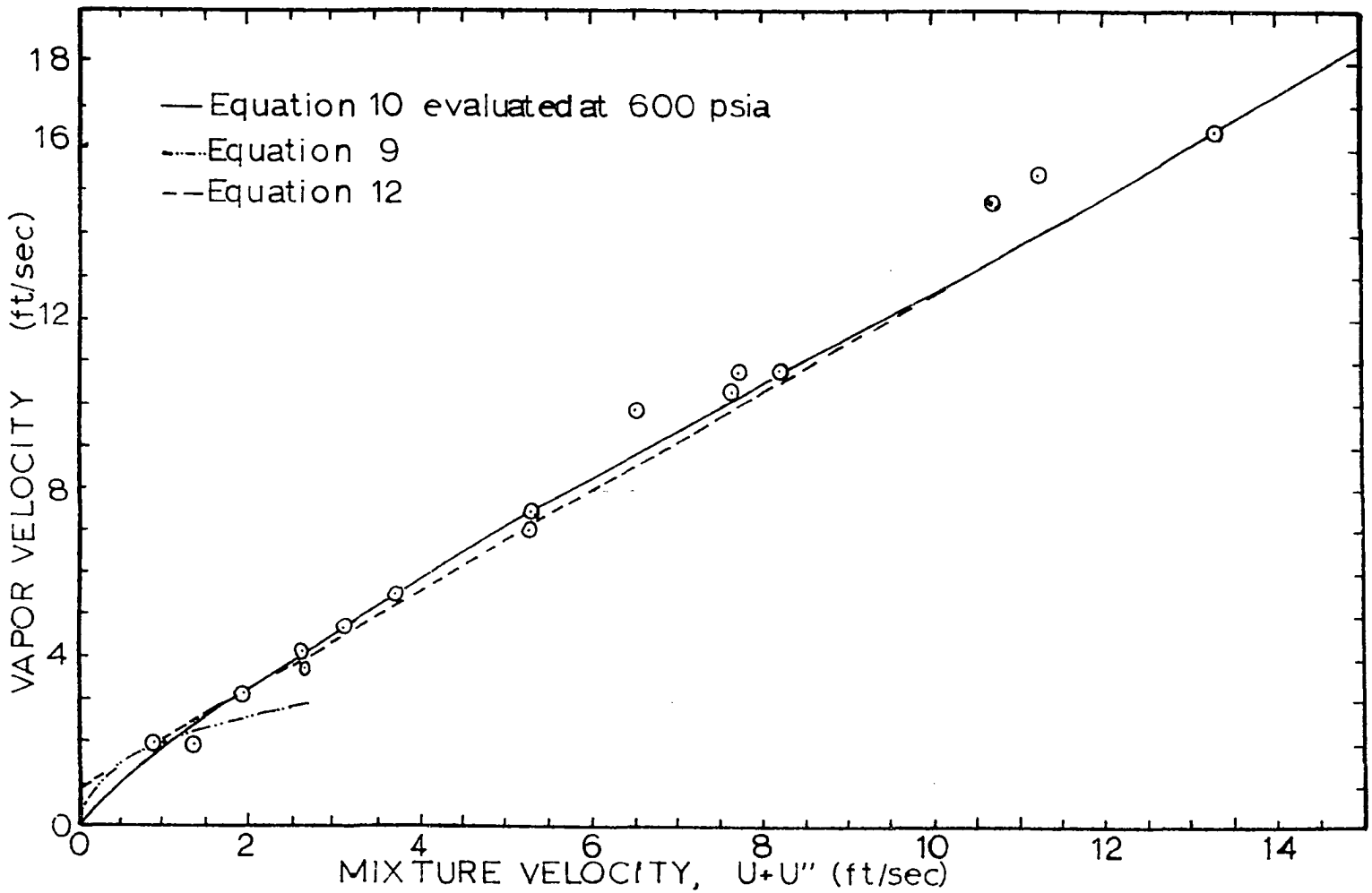

Figure 4. Relation between vapor velocity and mixture velocity

is negative (downward) and the magnitude of the liquid velocity is small in comparison to the magnitude of the bubble velocity. The void fraction would probably be less than 10%. In the second condition the value of V" would be nearly equal to that of a single bubble in a stationary liquid. Therefore, this value of V" is assumed to be a correct value when W is equal to zero under either condition described above.

The foregoing assumptions predict the bubble velocities for upward liquid flow, but little has been reported about slip velocities when the velocity of the liquid is downward. Wright (69) assumed that the slip ratio was the same in upward and downward flow when measuring heat transfer during forced downward two-phase flow. However, Wright had liquid velocities that were 30 to 40 feet per second which is many times greater than those encountered in this investigation. If the velocities of the liquid are large it is not unreasonable to assume that core flow results and that the velocity of the vapor is greater than that of the liquid. However, in this investigation the maximum downward liquid velocities are not expected to be greater than one or two feet per second if a two-phase mixture is flowing. At these low velocities the combination of Bernoulli and Magnus Forces have a tendency to concentrate the bubbles in an annular fashion. This would suggest that the relative velocity of the vapor at low velocities

would not differ greatly from that of a single bubble in a stationary fluid, or that the value of (V"-V) is constant. It is assumed that this relation describes the value of V" in the regions where W is less than zero.

The above procedure divides the two-phase flow relation into three regions.

1. W is much greater than zero and Kholodovskiy's equation applies.
2. W is slightly greater than zero and an empirical equation is used to correlate the values of V" and W which gives satisfactory values at W=0.
3. W is less than zero and the slip velocity of a single bubble is constant.

These three expressions may be written

$$\frac{U''}{\emptyset} = cW^n$$

$$\frac{U''}{\emptyset} = AW + B_1 \qquad 11$$

$$\frac{U''}{\emptyset} = W + B_2$$

The range of Kholodovskiy's equations where n = 0.84 suggests that this part of the curve might also be approximated by a straight line relation. This replaces one portion of Kholodovskiy's equation with another linear approximation and the curves with constants evaluated for 600 psi, become,

$$
\begin{aligned}
U'' &= 1.298\ \phi W^{0.981} && W \geq 11.65 \\
U'' &= \phi\ (1.16W + 0.96) && 0.266 < W \leq 11.65 \\
U'' &= \phi\ (2.85W + 0.51) && 0 < W < 0.266 \\
U'' &= \phi\ (W + 0.51) && W < 0
\end{aligned}
\qquad (12)
$$

The above approximations are plotted on Figure 5 .

The above modifications to Kholodovskiy's prediction equation thus give a series of equations for predicting the relationship between the two phases over a complete range of values for W. These equations appear to be in good agreement with observed data and will predict reasonable bubble velocities at all velocities except under divergent flow oscillations. This series of equations is probably the most critical item in predicting the behavior of two-phase flow. Examples of the variation of flow oscillation damping in calculated two-phase flow due to slight changes in the slip ratio are presented by Garlid (27).

B. Development of General Flow Equations

The purpose of this investigation is to determine the general behavior of a two-phase flow system and to gain some insight into the operation of a two-phase system from the behavior of a mathematical model. This is done by examining the non-linear flow equations with a digital computer and observing the behavior of the system. The non-linear flow

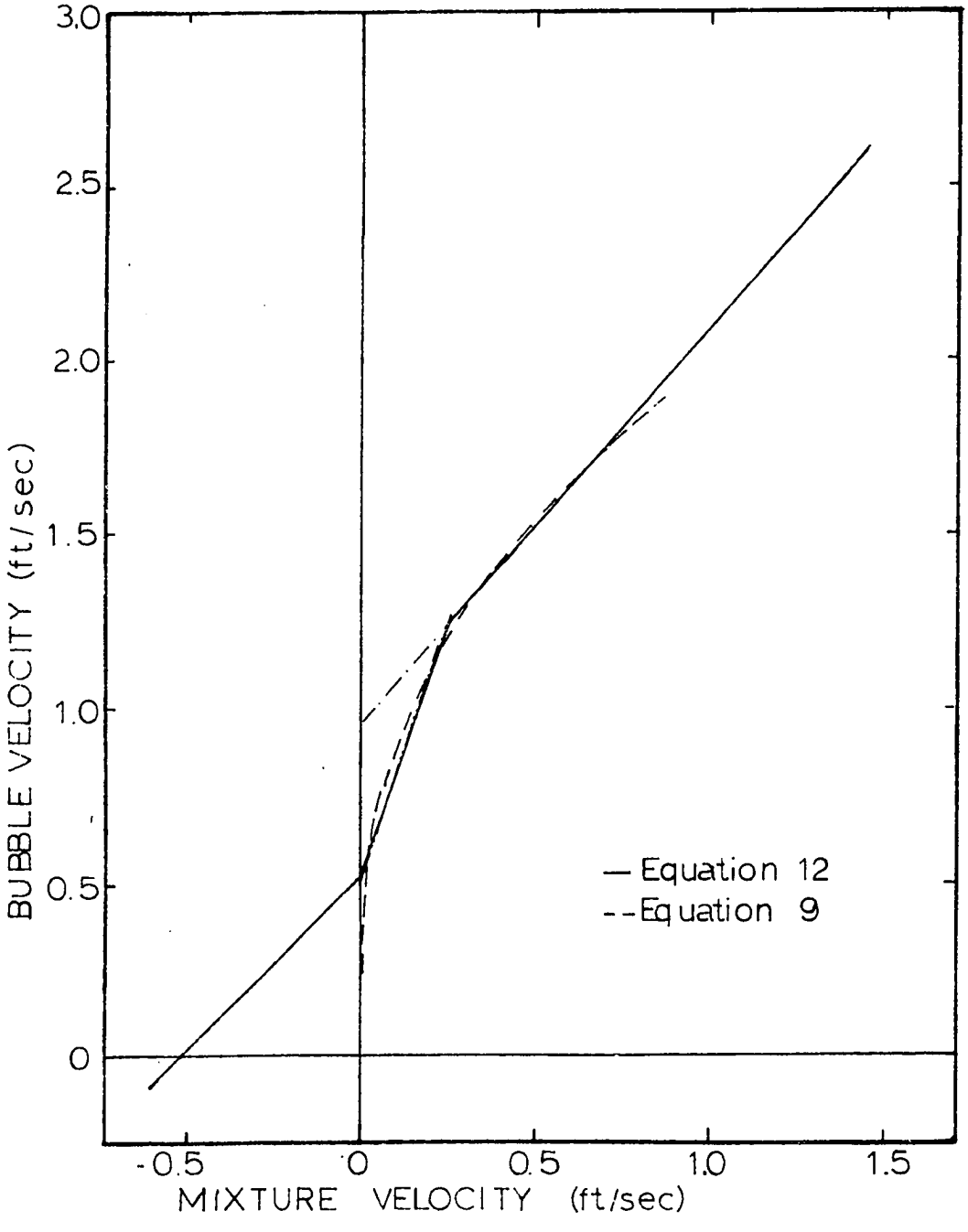

Figure 5. Modified flow relation at low velocities

system can have three types of behavior: stable, unstable, and oscillatory. The oscillatory type of behavior, which cannot be predicted if the equations are linearized (27), is the form of non-stable flow observed in most experimental tests because of the inherent damping that occurs in a fluid flow system.

The partial differential equations describing two-phase flow may be developed by applying the laws of the conservation of energy, mass, and momentum to a differential volume of a flow channel which contains a two-phase mixture (See Figure 6). It is assumed that the volume contains a mixture of liquid and vapor and each component occupies a distinct cross-sectional area. It is further assumed that at a cross-section the velocity of each phase is uniform throughout the area it occupies.

The mass flow rates through any unit area of the cross-section of a tube for the liquid and gas phases are given by the following equations.

$$G = (1-\emptyset)\,\rho V \qquad 13$$

$$G'' = \emptyset\, V''\, \rho'' \qquad 14$$

The resultant of all external forces applied to the volume shown in Figure 6 is equal to the time rate of change of the mass flow rate in this volume. If second order differentials are neglected this gives

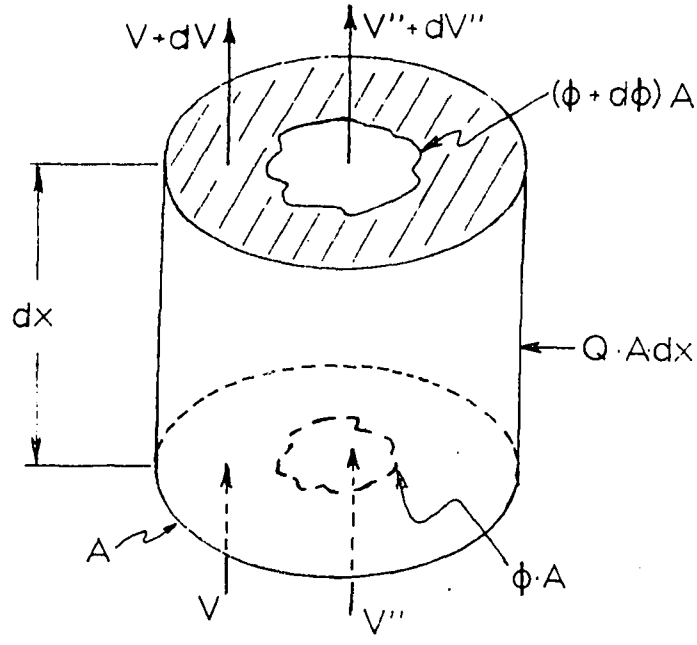

Figure 6. Differential volume of a two-phase mixture

$$dF = GV + G''V'' - (G + \frac{dG}{dx}\,dx)\,(V + \frac{dV}{dx}\,dx) - (G'' + \frac{dG''}{dx}\,dx)\,(V'' + \frac{dV''}{dx}\,dx) \qquad 15$$

When the change in mass flow is due only to a change of state the following holds.

$$-\frac{dG}{dx} = \frac{dG''}{dx} \qquad 16$$

Ignoring second order differentials and substituting Equation 16 into Equation 15, one obtains, after dividing by dx,

$$-\frac{dF}{dx} = G\frac{dV}{dx} + G''\frac{dV''}{dx} + (V''-V)\frac{dG''}{dx} \qquad 17$$

For unsteady flow the change in velocity with time is determined by the total derivative of the velocity

$$dV/dt = \frac{\partial V}{\partial t} + V\frac{\partial V}{\partial x} \qquad 18$$

Where the first term on the right side represents a change in velocity due to a change with time (the non-steady-state term) or the temporal acceleration, and the second term represents the convective change due to a change along the path of motion, which is called the spatial acceleration. Therefore, the full change in velocity along a section of a length with non-steady flow is equal to

$$\frac{dV}{dx} = \frac{dV}{dt} \cdot \frac{dt}{dx} = \frac{dV}{dt} \cdot \frac{1}{V}$$

$$= \frac{1}{V} \frac{\partial V}{\partial t} + \frac{\partial V}{\partial x} \qquad 19$$

Substituting the above relation for dV/dx and dV"/dx and using Equations 13 and 14 for G and G" respectively, one obtains

$$\frac{-dF}{dx} = (1-\emptyset)\rho \left(\frac{\partial V}{\partial t} + V \frac{\partial V}{\partial x}\right) + \emptyset \rho'' \left(\frac{\partial V''}{\partial t} + V'' \frac{\partial V''}{\partial x}\right)$$

$$+ (V'' - V) \frac{dG''}{dx} \qquad 20$$

The time rate of change of mass of a differential volume is the net sum of the mass flow rate into the element. For the differential volume this results in the equation of continuity for a two-phase flow which is

$$\frac{\partial}{\partial t} \left[(1-\emptyset)\rho\right] + \frac{\partial}{\partial x} \left[V(1-\emptyset)\rho\right] + \frac{\partial}{\partial t} (\emptyset \rho'') + \frac{\partial}{\partial x} (V \emptyset \rho'') = 0 \qquad 21$$

The first two terms represent the temporal and spatial mass changes in the liquid phase and the last two terms the corresponding changes in the vapor phase. Also the sum of the last two terms of Equation 21 is equal to the rate of change of mass per unit length, dG"/dx.

The respective forces acting on a differential length are the gravity, pressure, and friction forces. Substituting these forces for dF and the last terms of Equation 21 for

dG"/dx into Equation 20 one obtains a differential equation describing the motion of the differential element.

$$g(1-\emptyset)\rho + g\emptyset\rho'' - \frac{\partial P}{\partial x} - Fr = (1-\emptyset)\rho\left(\frac{\partial V}{\partial t} + V\frac{\partial V}{\partial x}\right)$$

$$+\emptyset\rho''\left(\frac{\partial V''}{\partial t} + V''\frac{\partial V''}{\partial x}\right) + (V''-V)\left[\frac{\partial}{\partial t}(\emptyset\rho'') + \frac{\partial}{\partial x}(V''\emptyset\rho'')\right] \qquad 22$$

In Equation 22 Fr is the friction per unit length which will be evaluated later. Equation 22 may also be expressed in terms of the reduced velocities of the components of the system. When this substitution is made and the equation is expanded for constant density components and rearranged, the following equation is obtained.

$$g(1-\emptyset)\rho + g\emptyset\rho'' - \frac{dP}{dx} - Fr = \rho\left(\frac{\partial U}{\partial t} + \frac{U}{1-\emptyset}\frac{\partial U}{\partial x}\right) + \rho''\left(\frac{\partial U''}{\partial t} + \frac{U''}{\emptyset}\frac{\partial U''}{\partial x}\right)$$

$$+ \left(\frac{\rho U}{1-\emptyset} - \frac{\rho'' U''}{\emptyset}\right)\frac{\partial \emptyset}{\partial t} + \left[\rho\left(\frac{U}{1-\emptyset}\right)^2 - \rho''\left(\frac{U''}{\emptyset}\right)^2\right]\frac{\partial \emptyset}{\partial x} \qquad 23$$

$$+ \rho''\left(\frac{U''}{\emptyset} - \frac{U}{1-\emptyset}\right)\left(\frac{\partial \emptyset}{\partial t} + \frac{\partial U''}{\partial x}\right)$$

The continuity equation may also be expressed in reduced velocities.

$$\frac{\partial \emptyset}{\partial t}(\rho'' - \rho) + \rho\frac{\partial U}{\partial x} + \rho''\frac{\partial U''}{\partial x} = 0 \qquad 24$$

When this is solved for $\frac{\partial \emptyset}{\partial t}$ and the resulting value substituted into Equation 23 one obtains after rearranging and collecting terms

$$g(1-\emptyset)\rho + g\emptyset\rho'' - \frac{\partial P}{\partial x} - Fr = \rho\frac{\partial U}{\partial t} + \rho''\frac{\partial U''}{\partial t} + 2\rho''\frac{U''}{\emptyset}\frac{\partial U''}{\partial x} + 2\rho\frac{U}{1-\emptyset}\frac{\partial U}{\partial x} + \left[\rho\left(\frac{U}{1-\emptyset}\right)^2 - \rho''\left(\frac{U''}{\emptyset}\right)^2\right]\frac{\partial \emptyset}{\partial x} \qquad 25$$

Equation 25 may be written

$$g(1-\emptyset)\rho + g\emptyset\rho'' - \frac{\partial P}{\partial x} - Fr = \rho\frac{\partial U}{\partial t} + \rho''\frac{\partial U''}{\partial t} + \frac{\partial}{\partial x}\left(\rho''\frac{U''^2}{\emptyset}\right) + \frac{\partial}{\partial x}\left(\rho\frac{U^2}{1-\emptyset}\right) \qquad 26$$

This is the complete differential equation describing the flow inside a vertical channel using reduced velocities.

Equation 26 has been derived from momentum and continuity conservation, and is valid for uniform motion of a two-phase system with incompressible components.

The conservation of energy equation, Equation 6, may also be written in terms of reduced velocities.

$$\frac{\partial}{\partial x}(h_v\rho''U'' + h_f\rho U) + \frac{\partial}{\partial t}(h_v\rho''\emptyset + h_f\rho(1-\emptyset)) - \frac{Q}{g} = 0 \qquad 27$$

When this is expanded for incompressible components

$$h_v\rho''\frac{\partial U''}{\partial x} + h_f\rho\frac{\partial U}{\partial x} + (h_v\rho'' - h_f\rho)\frac{\partial \emptyset}{\partial t} - \frac{Q}{g} = 0 \qquad 28$$

The continuity and energy equations may be combined to yield two useful equations,

$$\frac{\partial \phi}{\partial t} = \frac{\partial U}{\partial x} + \frac{Q}{\rho g h_{fg}}$$

$$\frac{\partial \phi}{\partial t} = -\frac{\partial U''}{\partial x} + \frac{Q}{\rho'' g h_{fg}} \qquad 29$$

Elimination of $\frac{\partial \phi}{\partial t}$ between these equations results in another useful expression

$$\frac{\partial U''}{\partial x} + \frac{\partial U}{\partial x} = \frac{Q v_{fg}}{h_{fg}}$$

or

$$\frac{\partial W}{\partial x} = \frac{Q v_{fg}}{h_{fg}} \qquad 30$$

Equations 26 and 28, when combined with the empirical equation describing the interaction between the two phases describe the behavior of the two-phase model used in this thesis. An analytical solution to these differential equations was not determined. They were solved by means of a digital computer as described in the next section.

The use of reduced velocities simplifies the expressions describing the flow. This is done at a possible sacrifice in a physical feeling for the events taking place. The reduced velocities contain both void and velocity terms and the actual liquid and vapor velocities are somewhat obscured. However, these parameters simplify the solution of the flow equations and the description of the interaction between the two phases.

VI. SOLUTION OF EQUATIONS

The equations developed in this thesis are similar to those used by George (28) and Garlid (27) for analyzing a simple loop, but differ in the parameters used to describe the flow. George did not solve for liquid or vapor velocities, but expressed the flow in terms of a single mass flow rate, and also calculated the density as an experimentally determined function of the steam quality. Garlid solved the equations in terms of liquid velocity and void fraction and assumed that the slip ratio was constant or that it varied linearly with the liquid velocity. The differential equations used in this thesis to describe the flow have two characteristics not found in any of the analyses surveyed.

1. The equations are expressed in terms of the reduced velocities of the components.
2. The relation between the liquid and vapor velocities is given by Kholodovskiy's (36) relationship, and this is modified to give values of the vapor when the liquid flow is zero or downward.

An analytical solution of the partial differential equations describing the system was not obtained because of the non-linear nature of the equations. The equations were solved by dividing the channels into a number of increments and using finite difference equations to reduce the partial differential equations to total differential equations. The

necessary integration and differentiation to solve these equations was done on a digital computer.

A. Assumptions

Seven important assumptions were made in solving these equations. Some of these have been previously mentioned and are repeated here for completeness.

1. It is assumed that all the heat generated is transferred to the two-phase mixture, and transferred with no time delay.

2. It is assumed that there is no boiling in the subcooled regions of the channel. The general effect of subcooled boiling is to add buoyancy, or reduce the average density of the riser leg. This occurs in a short section of the heated region. The overall average density change in the channel due to subcooled boiling is greatly reduced by the addition of the riser section above the heated section. Maurer (53) and Foglia (24)show experimental values for the voids in the saturated regions are not greatly affected by the subcooled boiling.

3. It is assumed that there is no carryunder of vapor in the downcomer. The effect of carryunder is to reduce the density of the fluid in the downcomer. This assumption would, to a certain degree, compensate for the second assumption. Little information is available about the carryunder of vapor.

In most systems the make up water is added at the top of the downcomer and this greatly reduces any carryunder of voids. A recent paper by Petrick (58a) indicates that there is a critical velocity at which carryunder will commence.

4. It is assumed that the relationship between the two phases is the same in steady and non-steady flow. The empirical equations that are used to relate the phases were derived from steady-state observations. Unfortunately, very little is known about the behavior of a two-phase system during transients or when the system is subject to an acceleration. However, the assumption that the behavior of the system would not be greatly affected by non-steady conditions may be intuitively justified by reasoning that the time for a bubble to achieve equilibrium is small in comparison to the time for an oscillation.

5. All fluid properties are evaluated at a common pressure.

6. Each phase of the fluid is considered to be incompressible. Under reasonable operating conditions the change in vapor density due to pressure change will be negligible. All vapor is at saturation temperature so there is no change in vapor density due to temperature changes.

7. The kinetic energy terms of the fluid are negligible in comparison to the enthalpy terms.

B. General Pressure Equations

A necessary condition at all times is that the total pressure change along the risers and the downcomers be the same. This is necessary since all are connected above and below by a common plenum.

The total pressure change along a channel may be found by multiplying Equation 23 by dx and integrating over the length of the channel. When this is done and the equation rearranged the following equation results:

$$P = g\int_o^L \rho\,(1-\emptyset)dx + g\int_o^L \rho''\emptyset dx + \int_o^L Fr\,dx + \int \rho \frac{\partial U}{\partial t}\,dx$$
$$+\int_o^L \rho''\frac{\partial U''}{\partial t}\,dx + \int_o^L \rho''\,\frac{d}{dx}\left(\frac{U''^2}{\emptyset}\right)dx + \int_o^L \frac{d}{dx}\left(\frac{U^2}{1-\emptyset}\right)dx \qquad 31$$

The first two terms on the right side represent the effect of gravity and may be evaluated by numerical integration if $\emptyset$ is known.

$$g\int_o^L\left[\rho(1-\emptyset)+\rho''\emptyset\right]dx = g\sum_{i=1}^{n}\left(\rho(1-\emptyset_i)+\rho''\emptyset_i\right)\Delta x_i \qquad 32$$

The last two terms on the right side of Equation 31 represent the pressure change due to convective or spatial acceleration and may be evaluated by the values of the function at the upper and lower limits. In the model analyzed a step change in the flow area between the heated section and the riser section necessitates integrating over each of these lengths

and the total spatial pressure change is the sum of the spatial pressure change occurring before the step change and that occurring after the change. The pressure drop across the step change is calculated in the friction losses. Thus for each section of the channel the pressure drop from the last terms of Equation 31 is given by

$$\int_o^L \frac{d}{dx}\left(\rho'' \frac{U''^2}{\emptyset} + \rho \frac{U^2}{1-\emptyset}\right) dx = \rho'' \frac{U''^2_i}{\emptyset_i} - \rho'' \frac{U''^2_o}{\emptyset_o} + \rho \frac{U_i^2}{1-\emptyset_i} - \rho \frac{U_o^2}{1-\emptyset_o} \qquad 33$$

where the subscripts i and o refer to the entrance and exit conditions respectively for each section. In Figure 9 there are two such sections for each channel.

The friction losses are determined from the Darcy-Weisbach formula and a multiplier, R, to allow for the increase in friction due to two-phase flow. Therefore, the third integral is evaluated as

$$\int_o^L F_r dx = \int_o^L R\, f \frac{V_o^2}{2d} \rho\, dx = \frac{\rho}{2d} \sum_{i=1}^{n} R_i f_i V_{oi}^2 \Delta x_i \qquad 34$$

The velocity V_o, in Equation 34 is the velocity the mass would have if the mass flow were occurring as a liquid. The methods of obtaining R and f are discussed in a later section of this thesis.

Also included in the friction losses are minor losses.

Minor losses would be introduced by entrance and exit effects, the change in the diameter or flow area, and by any obstructions in the flow path such as fuel pin supports. These are estimated to be two inlet velocity heads. This is a rather arbitrary value, but a precise description of the facility under investigation would be necessary to describe this term fully.

C. Temporal Acceleration Calculations

The two terms on the right side of Equation 31 which contain an unknown temporal acceleration term are the terms which predict the dynamic behavior of the system. The evaluation of these terms is the object of the computer program. It is not possible to assign a uniform acceleration to all nodes in a channel. It is necessary to determine the acceleration of each node in the channel to describe properly the behavior of the model.

The acceleration of the components at each node is dependent on the acceleration of the components at the lowest node and also on what is happening in all the other nodes. For example, an increase in boiling rate would be expected initially to increase the flow out the top of a channel and decrease the flow into the channel. Also an increase in flow rate at the lowest node would require an increase in exit rate if there were no change in voids in the system.

Equation 30, which was derived from the continuity and

energy equations, may be used to determine the value of the sum of U" and U at any point at a given time. When both sides of Equation 30 are multiplied by dx and the integration performed at a fixed time between the limits of zero and a point x the equation takes the form

$$U''_x + U_x = U''_1 + U_1 + \int_o^x \frac{QV_{fg}}{H_{fg}}\, dx \qquad 35$$

This equation gives the sum of the reduced liquid and reduced vapor velocities at a position x above the lowest node at any time as a function of the flow at the lowest node and the heat rate between the lowest node and the point. This equation may be differentiated with respect to time with the following result

$$\frac{\partial U''_x}{\partial t} + \frac{\partial U_x}{\partial t} = \frac{\partial U''_1}{\partial t} + \frac{\partial U_1}{\partial t} + \frac{V_{fg}}{H_{fg}} \int_o^x \dot{Q}\, dx \qquad 36$$

The value of U''_1 will be zero when the flow is upward because the fluid entering the lowest node contains no voids, and U" will be very small or zero for downward flow, with the possible exception of diverging flow oscillations. Therefore, in any flow condition expected to be found in a naturally circulating loop $\frac{\partial U''_1}{\partial t}$ will be zero or very small and this term can be dropped from Equation 36 and this equation becomes

$$\frac{\partial U_x}{\partial t} = \frac{\partial U_1}{\partial t} + \frac{V_{fg}}{H_{fg}} \int_o^x \dot{Q} dx - \frac{\partial U''x}{\partial t} \qquad 37$$

Equation 37 gives the acceleration of the reduced liquid at a position x as a function of the acceleration of the reduced liquid at the first node, the time rate of change of heat generation up to that node, and the acceleration of the reduced vapor at the position x.

The relationship between $\frac{\partial U''}{\partial x}$ and $\frac{\partial U}{\partial x}$ is determined from the empirical equations which relate the two-phase flow. They may be differentiated with respect to time to yield

$$\frac{\partial U''}{\partial t} = nc\phi W^{n-1} \frac{\partial W}{\partial t} + c\phi W^n \frac{\partial \phi}{\partial t} \qquad 38\text{-a}$$

$$\frac{\partial U''}{\partial t} = A\phi \frac{\partial W}{\partial t} + (AW+B) \frac{\partial \phi}{\partial t} \qquad 38\text{-b}$$

The first equation is in the region where the flow relationship is governed by Kholodovskiy's equation, and the second equation where the flow relationship is in the linear region. Equation 37 may be written

$$\frac{\partial W}{\partial x} = \frac{\partial U_1}{\partial t} + \frac{V_{fg}}{H_{fg}} \int_o^x \dot{Q} dx \qquad 37\text{-a}$$

and substitution of this value for $\frac{\partial W}{\partial x}$ into Equations 38-a and 38-b yields

$$\frac{\partial U''_x}{\partial t} = nc\phi_x W_x^{n-1} \left(\frac{\partial U_1}{\partial t} + \frac{V_{fg}}{H_{fg}} \int_o^x \dot{Q}dx\right) + cW_x^n \frac{\partial \phi x}{\partial t} \qquad 39\text{-a}$$

$$\frac{\partial U''_x}{\partial t} = A\phi_x \left(\frac{\partial U}{\partial t} + \frac{V_{fg}}{H_{fg}} \int_o^x \dot{Q}dx\right) + (AW+B) \frac{\partial \phi x}{\partial t} \qquad 39\text{-b}$$

Equations 39-a and 39-b express $\frac{\partial U''_x}{\partial t}$ as a function of $\frac{\partial U_1}{\partial t}$, $\frac{\partial \phi_x}{\partial t}$, the time rate of change of heat generation and the flow conditions existing at point x.

Equations 37 may be substituted for $\frac{\partial U}{\partial t}$ on the right side of Equation 31. After the results are rearranged the two integrals on the right side of Equation 31 which contain spatial acceleration terms take the form

$$\int_o^L \left(\rho \frac{\partial U}{\partial t} + \rho'' \frac{\partial U''}{\partial t}\right) dx = \int_o^L \rho \left(\frac{\partial U_1}{\partial t} + \frac{V_{fg}}{H_{fg}} \int_o^{x_i} \dot{Q}dx\right)dx - \int_o^L (\rho - \rho'') \frac{\partial U''}{\partial t} dx \qquad 40$$

When the value of $\frac{\partial U''}{\partial t}$ in Equations 39 is substituted into Equation 40, and the total value of the integral in Equation 40 is set equal to I

$$I = \int_o^L F_1 (W,\phi) \frac{\partial U_1}{\partial t} dx + \int_o^L \left\{ \int_o^x F_2 (W,\phi,\dot{Q})dx \right\} dx - \int_o^L (\rho - \rho'') \frac{U''}{\phi} \frac{\partial \phi}{\partial t} dx \qquad 41$$

where

$$F_1(W,\emptyset) = \rho(1-nc\emptyset W^{n-1}) + \rho'' nc\emptyset W^{n-1} \qquad W \geq W_{cr}$$

$$F_1(W,\emptyset) = \rho(1-A\emptyset) + \rho''A\emptyset \qquad W \leq W_{cr} \qquad 42$$

and

$$F_2(W,\emptyset,\dot{Q}) = \dot{Q}\left[\rho(1-nc\emptyset W^{n-1}) + \rho'' nc\emptyset W^{n-1}\right]\frac{V_{fg}}{H_{fg}} \qquad W \geq W_{cr}$$

$$F_2(W,\emptyset,\dot{Q}) = \dot{Q}\left[\rho(1-A\emptyset) + A\emptyset\rho''\right]\frac{V_{fg}}{H_{fg}} \qquad W < W_{cr}$$

43

Where W_{cr} is the value of W where the flow equation becomes non-linear in W. In the region where W is less than W_{cr} the proper value of A in Equations 42 and 43 is determined by Equation 12.

Nomenclature may be somewhat simplified by letting the three integrals on the right side of Equation 41 be I_1, I_2, and I_3. Thus

$$I = I_1 + I_2 - I_3$$

The three integrals on the right side of Equation 41 may be evaluated by numerical integration. To evaluate the first integral it is noted that $\frac{\partial U_1}{\partial t}$ is a constant for a given channel at a particular time. This may be moved outside the integral and the resulting equation may then be numerically integrated giving

$$I_1 = \frac{\partial U_1}{\partial t} \sum_{i=1}^{n} F_1 (W,\emptyset)\, R_i \Delta x_i \qquad 44$$

Where the value of F_1 at each node is given by Equation 42 and $R_i = 1$ in the region below the step increase in area, and $R_i = \frac{\text{Area (1)}}{\text{Area } (i)}$ if i is greater than $i = z$, where z is used to designate the last node with the same flow area as that in the first node. This assumes that the flow at the change in area is incompressible and there is no phase change in going through the step increase. When the summation process is carried out the integral takes the form

$$I_1 = K_1 \frac{\partial U_1}{\partial t} \qquad 45$$

The second integral will also be evaluated by numerical integration. For the case of steady heating rate the value of the integral will be zero. When the heating rate is not steady, but is known, the second integral takes the form

$$I_2 = \frac{Vfg}{Hfg} \sum_{i=1}^{n} R_i \left(\sum_{j=1}^{i} F_2(W,\not{\emptyset},\dot{Q}) \Delta x_j \right) \Delta x_i \qquad 46$$

R_i is evaluated as in Equation 44. The inner series represents the function given by Equation 43. The terms in the inner series will have non-zero values only in the region where boiling has started, and the terms will be zero where no heat is generated. Equation 46 represents a pressure change in the column due to accelerations induced by a change

in the rate voids are generated in the column.

The third integral in Equation 41 may also be evaluated by numerical integration. The value of $\frac{\partial \phi}{\partial t}$ is determined from the relation given by Equation 29 and the integral may be represented by

$$I_3 = (\rho - \rho'') \sum_{i=1}^{n} F_3 \left(U''_i, \phi_i, \frac{\partial \phi_i}{\partial t}\right) \Delta x_i$$

where $F_3 = 0$ if $\phi = 0$ and $F_3 = \frac{U''}{\phi} \frac{\partial \phi}{\partial t}$ if $\phi > 0$ 47

Grouping all the terms on the right side of Equation 31 now results in an equation of the form $P = K_1 \frac{\partial U_1}{\partial t} + B$, where B represents pressure changes due to friction, gravity, spatial acceleration, change in heating rate, and change in void generation, and K_1 is the constant found from Equation 44. A similar expression may be found for the pressure drop across the other channel.

The pressure drop across the downcomer can also be evaluated. If the downcomer is of constant area and no voids the only terms occurring in the downcomer pressure drop will be terms due to gravity, friction, and temporal acceleration, and it will not be necessary to integrate over the downcomer region.

Since the pressure drop across each channel and across the downcomer must be equal the equations describing this pressure drop across each channel may be set equal to each other. When the common pressure drop is eliminated from

these three equations there remain two equations in three unknowns--the temporal accelerations of the first node of the two risers and the acceleration of the downcomer. A third equation relating the acceleration of the columns may be obtained by applying the continuity equation to the region below the channels. This results in three equations in three unknowns which take the general form

$$K_{1,j}\frac{\partial U_{1,j}}{\partial t} + B_j - K_3\frac{\partial U_3}{\partial t} + B_3 = 0 \qquad j = 1,2 \qquad 48\text{-a,b}$$

where j refers to the values for the two risers and

$$\text{Area (1)}\frac{\partial U_{1,1}}{\partial t} + \text{Area (2)}\frac{\partial U_{1,2}}{\partial t} = \text{Area (3)}\frac{\partial U_3}{\partial t} \qquad 48\text{-c}$$

(The positive direction for U_3 is down or into the lower plenum, and the positive direction for $U_{1,1}$ and $U_{1,2}$ is upward or out of the lower plenum.)

These three equations may be solved simultaneously to determine the value of the acceleration of the lowest node in each riser and the acceleration of the liquid in the downcomer.

The time rate of change of voids at each node is determined from Equation 29. Thus, after a time interval ΔT it is possible to predict the value of voids by the equation

$$\emptyset_{i,j,k+\Delta T} = \emptyset_{i,j,k} + \frac{\partial \emptyset}{\partial t}\Delta T \qquad 49$$

Where k is time index, i the node, and j the channel, and $\frac{\partial \emptyset}{\partial t}$ is given from Equation 29 and the procedure to calculate $\frac{\partial \emptyset}{\partial t}$ in Equation 29 is discussed in the next section.

A value for W at the first node after a time interval ΔT is calculated by

$$W_{i,j,k+\Delta T} = W_{i,j,k} + \frac{\partial U_{1,j}}{\partial t} \cdot \Delta T \qquad 50$$

It is possible to calculate the value of W at all node points by integrating Equation 44.

$$W_x = W_1 + \int_0^x \frac{QV_{fg}}{H_{fg}} \, dx$$

or

$$W_x = W_1 + \sum_{i=1}^{x} \frac{Q_i V_{fg}}{H_{fg}} \Delta x_i \qquad 51.$$

New values for U" are now calculated at each node using the new values for W and $\emptyset$ at each node found from Equations 49 and 51 and the proper form of Equation 11. The new value of U is then determined at each node from the relation U=W-U".

The above procedure produces new values for U, U", and $\emptyset$ at all nodes and the calculation process is repeated for a new time increment.

D. Summary of Calculation Procedures

The complete calculation sequence is summarized as follows:

1. An initial set of flow conditions are given to each node in each channel. These flow conditions satisfy the

relationship between the two phases given by Equation 11.

2. The time rate of change of voids at each node is calculated from the equation $\frac{\partial \emptyset}{\partial t} = \frac{-\partial U''}{\partial x} + \frac{Q}{\rho'' g H_{fg}}$.

The space derivative of U" is calculated using forward differencing techniques as described in a following section.

3. The pressure drop across each channel is determined as a function of the temporal acceleration of the lowest node, the reduced liquid and vapor velocities, the void fractions, the time rate of change of voids, the time rate of change of heat generation rate, and the fluid friction.

4. The acceleration of the liquid at the lowest node of each channel is determined by solving the equations found in step three with the continuity equation for the lower region of the loop.

5. New values for the voids at all nodes in all channels are calculated for a time step after the initial conditions.

6. New values for W, U and U" are calculated for the lowest, or first, node in each channel for a time step after the initial conditions.

7. New values for W, U" and U are calculated for all remaining nodes in that order by integrating Equation 30 to obtain new values of W at all nodes, using Equation 11 and the new value of voids at each node to determine the new value of U" and using the definition of W to calculate the new value

of U.

8. Determine the maximum permissible time step for the next time increment. The procedure for doing this is discussed in the next section.

9. Perform miscellaneous calculations which are unique to the system under study. This includes such things as

   a. Calculate change of heat generation rate and determination of the time rate of change of heat generation rate.

   b. Printing of calculated data.

10. Repeat the above sequence for a specified amount of time.

E. Calculation of the Point Where Boiling Starts

In any calculation involving heat generation it was necessary to determine whether or not boiling occurred before applying the proper equations. In regions of no vapor generation the terms involving Q and $\dot{Q}$ are zero--the heat is used to raise the temperature of the water and does not produce a phase change. The point where boiling starts when the flow is upward is determined by calculating the enthalpy of the liquid at each node by the equation

$$h_i = h_{i-1} + \frac{Q_{i-1}\ (\Delta x_i)}{\rho\ g\ V}$$

Q_{i-1} is the heat generation rate between the node i and the

node i-1. For the first node h_i is set equal to enthalpy of the subcooled liquid in the plenum below the risers.

When h_i is less than the enthalpy of the saturated liquid the terms involving Q are set equal to zero in all calculations for the node i. At the first node where the value of h_i is greater than the enthalpy of the saturated liquid the terms involving heat generation are evaluated, but only the fraction of the heat in that node that produces vapor is used as the value for Q in the calculations. For all nodes above the first node where h_i is greater than the enthalpy of the saturated liquid the terms involving Q are evaluated and it is assumed that all the heat is used to produce a change in phase.

The above procedure calculates the point where boiling starts if the liquid velocity is constant. A special case can arise during a transient in which the velocity is increasing. This acceleration could result in voids being present in a node where the calculated enthalpy, which assumes constant velocity, is less than the enthalpy of the saturated liquid. When this occurs the change in voids due to heat generation is assumed to be equal to zero at the first node that contains voids and for all subsequent nodes the terms involving Q are calculated. This means that a rapid increase in flow can only "sweep" the voids from a single node during a single time interval, and that the phase change due to heat generation

will continue in all nodes above this node until the voids are removed.

When the flow is downward it is assumed that the liquid is saturated at all nodes and that all the heat is producing a change in the two-phase flow. The choice of value for Q when the flow is downward is discussed in the section on computer techniques.

The above routine explains the general calculation procedure. A flow chart for the computer program is shown in Figure 8 .

F. Friction Losses

The steady-state circulation rate of a naturally circulating boiling loop is determined by a balance between the buoyant forces (caused by a phase change) which produce the driving force, and the drag forces which are caused by friction on the channel boundaries and the forces necessary to produce the spatial acceleration of the liquid phase in the boiling region.

The single-phase flow drag loss is usually calculated by using the Darcy-Weisbach equation.

$$H_L = f \frac{l}{d} \frac{V^2}{2g} \qquad 52$$

where H_L is the head loss, or

$$\Delta P = f \frac{l}{2d} V^2 \qquad 53$$

For two-phase flow the friction factor f, which is the friction factor if liquid only were flowing, is multiplied by a factor R which is the ratio between two-phase friction loss and the friction loss if the fluid were liquid only. When the multiplier R is used the velocity term in Equation 52 is the velocity the system would have if all the flow were liquid, and the density is the liquid density.

The friction factor, f, was calculated using Blasius's well-known equation (65) for friction factors in a smooth pipe.

$$f = \frac{0.316}{(Re)^{0.25}} \qquad 54$$

For low flows the value of f was set equal to 0.012.

Considerable work has been done towards determining the friction multiplier. The most well-known work is the Martinelli-Nelson correlation, and this has been the guide for most friction factor determinations in two-phase flow. Recent observers have tended to arrive at less elaborate methods of determining the two-phase multiplier. The Lottes-Flinn (50) correlation describes the two-phase friction factor by the following equation

$$R = \frac{1}{3}\left[1 + \frac{1}{1-\emptyset} + \left(\frac{1}{1-\emptyset}\right)^2\right] \qquad 55$$

Observed friction factors on natural circulation loops have led Anderson *et al.* (2) to use the empirical equation for EBWR friction multipliers

$$R = \frac{K}{(1-\emptyset)^2} \qquad 56$$

where K is 1.0 for regions of no heat generation, and 1.3 for regions of heat generation.

The last two equations obviously fail to satisfy the flow equations for high void fractions because of the $(1-\emptyset)$ factor in the denominator of each expression, but they are generally valid for flow up to about 60 percent voids.

The friction factor is not specified in the development of the general flow equations. The geometry used to determine the behavior of a model was similar to EBWR geometry. For this reason the friction factor recommended by Anderson was used for voids less than 60%, and for voids greater than this it was assumed that the friction factor multiplier varied linearly as a function of voids between the value at 60% and the friction factor multiplier that would occur if only vapor were flowing.

The friction factor multiplier is calculated in a special section of the computer program and modification of the calculation procedure to accommodate a particular system if experimental data are available would be a simple procedure.

G. Computer Techniques with Finite Difference Equations

In this thesis the partial differential equations describing the flow are reduced to total derivatives in time by replacing the space derivatives with finite difference

equations. Using this method the equation for change of voids at a node is given by

$$\frac{d\emptyset_i}{dt} = - \frac{\Delta U''}{\Delta x} + \frac{Q_i}{\rho'' \cdot H_{fg} \cdot g}$$

where $\frac{\partial U''}{\partial x}$ in Equation 29 has been replaced by $\frac{\Delta U''}{\Delta x}$, and $\frac{\Delta U''}{\Delta x}$ is calculated with difference equations. The calculated behavior of the system is very sensitive to the method used to calculate $\frac{\Delta U''}{\Delta x}$.

Figure 7 shows a typical node in a one-dimensional space grid. The simple method to calculate $\frac{\Delta U''}{\Delta x}$ at the node i is

$$\frac{\Delta U''}{\Delta x} = \frac{U''_{i+1} - U''_{i-1}}{2 \Delta x} \qquad 57$$

This is the same relation obtained if the values of U'' at $i - \frac{1}{2}\Delta x$ and $i + \frac{1}{2}\Delta x$ are averaged at the mid point of the nodes by a trapezoidal rule, and also the same result obtained if a quadratic equation is fitted to the values of U'' at $i - \Delta x$, $i + x$, and i, and the resulting quadratic equation evaluated at i. This differencing technique does not, however, produce a numerically stable solution when the equations are solved on a digital computer. Calculations using this technique produced a divergent saw tooth pattern for voids. The cause of this divergence was not determined.

Numerical stability in the digital computer solution of the equations was achieved by the use of forward and backward

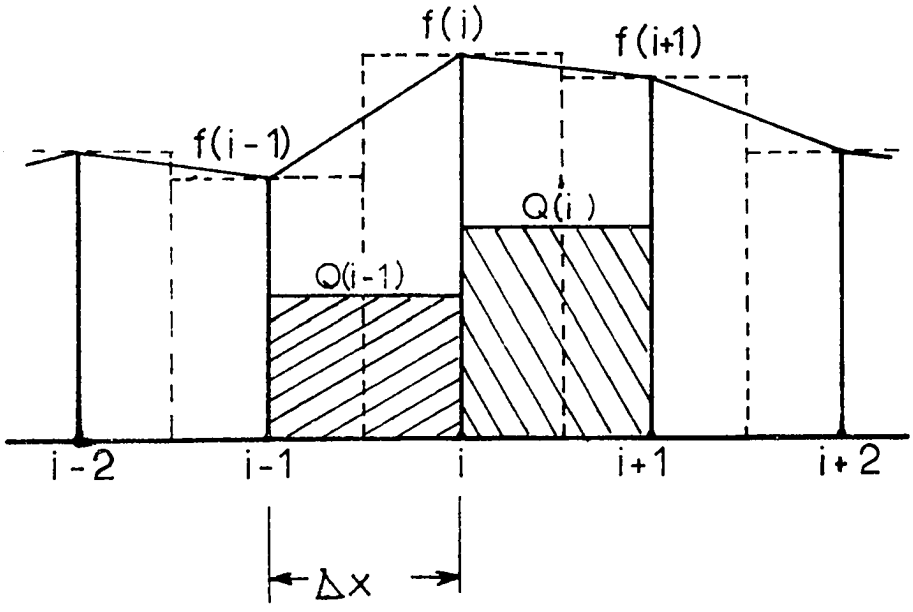

Figure 7.

Typical one-dimensional grid

differencing techniques to evaluate the space derivatives. In this method the value of $\frac{\Delta U''}{\Delta x}$ is given by

$$\frac{\Delta U''}{\Delta x} = \frac{U''_{i} - U''_{i-1}}{\Delta x} \qquad U'' > 0$$

$$\frac{\Delta U''}{\Delta x} = \frac{U''_{i+1} - U''_{i}}{\Delta x} \qquad U'' < 0 \qquad 58$$

The above equations may be explained by an intuitive reasoning process. The use of nodes implies that the value of $\emptyset$ at i represents the average value of $\emptyset$ between $i+\frac{1}{2}\Delta x$ and $i-\frac{1}{2}\Delta x$. The average value of $\frac{\partial U''}{\partial x}$ at the node i during the time interval will, from the mean value theorem, be between $\frac{\partial U''}{\partial x}_{i,j,k+\Delta\tau}$ and $\frac{\partial U''}{\partial x}_{i,j,k}$, and if the flow is to the right the value of $\frac{\partial U''}{\partial x}_{i,j,k+\Delta\tau}$ is dependent on the flow profile in the region to the left of node i at the initial time. During the time interval ΔT some of the fluid in node $i-1$ will flow into node i, and some of the fluid in node i will flow into the node $i+1$. Thus the average time rate of change of voids in the volume represented by i during the time interval ΔT will not be effected by the value of U''_{i+1} if the flow is to the right, but the value of U''_{i-1} will have an effect on the average time rate of change of voids in node i during this time interval. If the flow is to the left the same reasoning may be applied and the value of the derivative is given by the second equation above.

For the special case where the void fraction is greater than zero and $U''_i = 0$, the value of $\frac{\Delta U''}{\Delta x}$ is set equal to zero at the node i. This is a unique situation, and when it does occur the average value of $\frac{\partial U''}{\partial x}$ in an increment will be very nearly zero at the node during the time interval even for the most divergent oscillations.

Equation 58 is numerically stable when the program is solved on a digital computer. Longly (47) shows that this type of differencing introduces a second order diffusion effect. For $U'' > 0$, $\frac{U''_i - U''_{i-1}}{\Delta x}$ would represent the value of a $\frac{\partial U''}{\partial x}$ at $i-\frac{1}{2}\Delta x$. A Taylor expansion of a function f',

$$f'(x+\delta) = f'(x) + \delta f''(x) + \frac{\delta^2}{2} f'''(x)....$$

yields $f'(i-\frac{1}{2}\Delta x) = f'(i) - \frac{\Delta x}{2} f''(i)$

where only first and second order terms are used in the expansion. Correspondingly, for $U''_i < 0$

$$f(i+\frac{1}{2}\Delta x) = f(i) + \frac{\Delta x}{2} f''(i).$$

Another stability requirement in this type of differencing is that the time increment, ΔT, be less than the time required for a particle to move between two nodes. Richtmeyer (61, p 9) demonstrates the type of instability occurring if this law is violated, and Longly (47) indicates that for good accuracy the time increment should be about one-tenth this value. However, Longly was examining a shock wave and the acceleration in his

calculations were much greater than anything found in a naturally circulating loop.

In two-phase flow the velocity of each phase must be considered. In this program the time increment was selected as smallest value for any node of

$$\Delta T = 0.9 \left| \frac{\Delta x_i}{V_i} \right| \qquad \text{if } \emptyset = 0$$

or

$$\Delta T = 0.9 \left| \frac{\Delta x_i}{V_i''} \right| \qquad \text{if } \emptyset > 0 \qquad (59)$$

The selection of the grid size and the time increment must be a compromise between accuracy and economy. A very fine grid results in a large number of nodes and very small time increments, and hence greater accuracy at the expense of a two-fold increase in computer time. A coarse grid greatly reduces the number of calculations and increases the permissible time step at the expense of accuracy.

A technique similar to that used to determine the value of $\frac{\Delta U''}{\Delta x}$ is used to determine the value of heat input, Q, in Equation 29. The value of Q_i is the heat generation rate between the node i, and the node $i-1$. This does not represent the average value of heat generation at a differential volume centered around the node. In calculating the change in voids at the node i the term used for Q in Equation 29 is

$$Q = Q_{i-1} \qquad U > 0$$

$$Q = Q_i \qquad U \leq 0 \qquad (60)$$

Similarly, if the flow is upward, the value of Q used in determining the change in enthalpy between the node i and i-1 given by Equation 60.

The value of Q used in performing the numerical integration to determine W in Equation 51 and step 7 of the calculation procedure is the value between the nodes for both upward and downward flow. The values of Q used in pressure drop calculations are also evaluated at the same value for forward and reversed flow.

H. Change in Flow Area Calculations

In a boiling water reactor which has a riser above the heated region there is a sudden change in flow area between the fuel region and the riser. In this model the change in area was assumed to be a step change and this abrupt change in area required a number of special calculations. Some of these are outlined below. In this description of the calculation procedures the last node before the increase in flow area is designated as z and the first node with the increased flow area becomes z + 1.

During upward flow the time rate of change of voids at i = z + 1 was calculated from Equation 29 with the value of $\frac{\partial U''}{\partial x}$ given by a modified form of Equation 34.

$$\frac{\partial U''_{z+1}}{\partial x} = \frac{U''_{z+1} - U''_{z} \frac{A_z}{A_{z\,1}}}{\Delta x}$$

This equation modifies the reduced velocity of the vapor into the element so that it is the value the vapor phase would have if it were flowing in the larger flow area.

In the pressure drop calculations the terms involving friction and gravity are not affected by the change in flow area. The spatial acceleration terms, as previously mentioned, are divided into two sections, the section below the area increase and the section above the area increase. The pressure drop across the increase in area is included in minor loss calculations.

The temporal acceleration pressure drop terms require special calculations. The temporal acceleration pressure drop is calculated as a function of the acceleration of the lowest node and the time rate of change of heat generation and voids in the system. In the numerical integration of Equations 36 and 46 (which calculate the pressure drop due to the acceleration of the lowest node and a change in heating rate) the value of each term in the summation where $i > z$ was multiplied by the area ratio. This assumes that the fluid passes through the expansion as an incompressible fluid and that the acceleration of the fluid is inversely proportional to the flow area. Equation 47 is not corrected for the nodes above $i = z$ because this term involves changes at the node under consideration and is not affected by a change in area.

The calculation of the velocities of the components at

$i = z + 1$ is done by requiring continuity of mass flow between $i = z$ and $i = z + 1$. The exit flow from node z,

$$A_z \left(\rho U_z + \rho "U"_z \right) = G_z , \qquad 61$$

is set equal to the flow at node $z + 1$

$$A_{z+1} \left(\rho U_{z+1} + \rho "U"_{z+1} \right) = G_{z+1} = G_z . \qquad 62$$

The relation between $U"_{z+1}$ and U_{z+1} is determined by setting $W_{z+1} = \frac{A_z}{A_{z+1}} \cdot W_z$

The above equation predicts which one of the Equations 12 to use in relating U" and U. This equation is then solved simultaneously with Equation 62 to predict new values for $U"_{z+1}$ and U_{z+1}, and W_{z+1} is then set equal to

$U"_{z+1} + U_{z+1}$.

The method described above insures continuity of mass in the flow between nodes z and z+1. However, this method results in a slight discontinuity of flow for each phase as that phase goes past the increase in flow area (less than 1% for velocities tested). This error is small and would have very little effect on the flow velocities. The value of voids at the node z+1 decreases due to the flow area increase.

I. Computer Program

A digital computer program was written to perform the calculations outlined on the preceeding pages. This program was written in Fortran machine language and adapted for the IBM 7074 digital computer at the Iowa State University Computational Center. A general flow diagram for the computer program is shown in Figure 8 . This program performs the calculations to determine the time dependent behavior of the system after a set of initial flow conditions are imposed.

Before the repetitive flow-time calculations are performed it is necessary to input certain data describing the system which is being analyzed. The input data which must be given to the computer before calculations begin includes geometric parameters, pressure parameters, and initial flow conditions. Geometric parameters that are included in the input are

1. Flow areas in channels and downcomer
2. Equivalent diameters of flow areas
3. Number and spacing of nodes, and the node where change in flow area occurs

Initial flow conditions that are included in the input are

1. Reduced liquid and vapor velocities at all nodes
2. Void fractions at all nodes
3. Initial heat generation rates
4. Enthalpy of liquid in lower plenum

Pressure parameters that are included in the input are

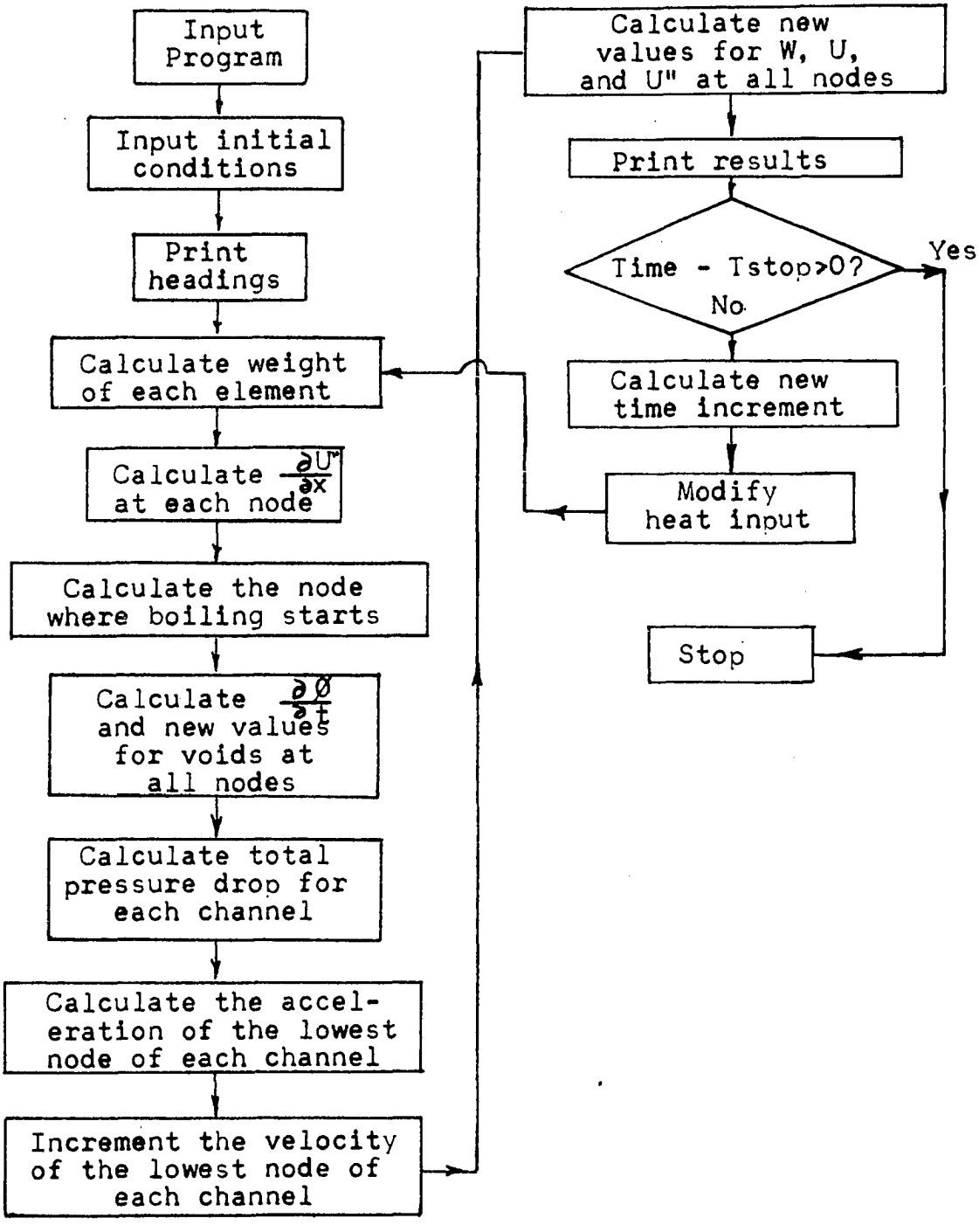

Figure 8. Flow diagram for digital computer program

1. Liquid and vapor densities and enthalpies
2. Pressure dependent constants associated with the Equation 11

The variation of one of the sets of parameters discussed permits investigation of the effect of the set of parameters on the flow system. Thus, it is possible to determine the effect of pressure by changing the set of cards associated with pressure. Also a different geometric model or set of initial conditions can be investigated by changing the cards associated with these parameters.

The variation of certain parameters with time, such as heating rates, is accomplished by a separate calculation section in the main calculation routine. This separate calculation routine can be altered without changing the main program, thus permitting the use of different heat generation rates or the time variation of the heat generation rate without altering other calculations.

The digital computer program contains about 500 cards and is omitted here for brevity. A copy is available in the Nuclear Engineering Reading Room.

VII. RESULTS

The true test of the mathematical model and the digital computer solution of the equations is how well they will predict the behavior of an actual system. No experimental data were found which would describe the behavior of a system similar to that described in this thesis. However, considerable data are available on the transient behavior of the Experimental Boiling Water Reactor and a system similar to this was investigated.

Figure 9 shows the system analyzed. This is similar to the EBWR after its modification for 100 MW operation. The two distinct channels do exist in the EBWR and the two riser channels in the model are the approximate shape of the two channels in the EBWR. In the EBWR the two heated regions have approximately the same heat generation rate, but in the model it is assumed that the two heated regions can have distinct differences in the heat generation rate. In the model each channel was divided into 22 nodes with a space increment of 6 inches between nodes. This spacing was a compromise between accuracy and computational time. The heat input into the heated region (the region between nodes 3 and 11) was in the form of a chopped cosine curve. The general form of the heat input was not changed during the experimental program, but the magnitude of the heat generation was varied. The model is compared to the EBWR in Table I.

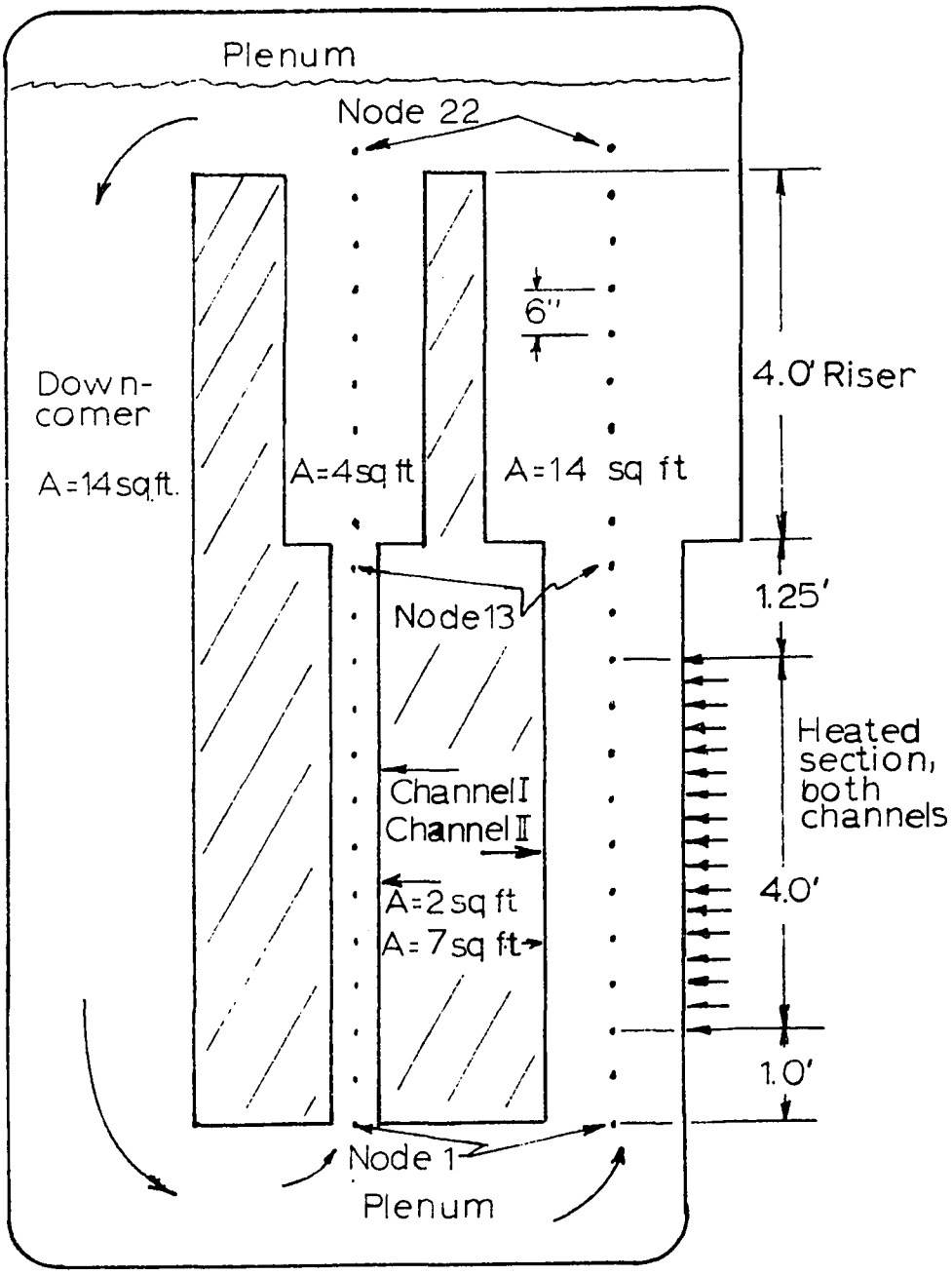

Figure 9. Details of model

A series of digital computer runs were made to determine the behavior of the system under constant and transient heat generation rates. The testing program can be divided into three phases

1. Behavior under steady heat generation rates and under ramp changes in heat generation rates. This provided a basis for determining whether or not the model provided reasonable steady-state flow values, since these could be compared with the EBWR flow rates.

2. Response of the system to step changes in one channel. The purpose of this phase of the program was to determine whether or not sustained flow oscillations could be triggered in one channel while the other channel remained stable. This would include flow reversals in one channel.

3. Response of the system to sinusoidal power oscillations in one channel. The purpose of this phase of the investigation was to determine whether or not the system had a critical frequency at which the flow would show a maximum response.

Table II is a tabulation of the various power conditions that were analyzed.

During most of the testing the liquid had an inlet velocity of about 4.5 feet per second and the exit voids fraction was about 45%. Under these conditions the time increment was about 0.032 seconds and the IBM 7074 computer required

Table 1. Comparison of EBWR and model

	EBWR[a]			Model		
	central region	outer region	down-comer	Channel I	Channel II	down-comer
Total length (ft)	9.0	9.0	9.0	10.125	10.125	10.125
Core length (ft)	6.0	6.0		6.125	6.125	
Heated section (ft)	4.0	4.0		4.0	4.0	
Riser length (ft)	3.0	3.0		4.0	4.0	
Flow area (sq ft)			13.305			14.000
Core	1.865	6.701		2.0	7.0	
Risers	4.0	12.44		4.0	14.0	
Equivalent diameter (ft)			1.412			1.412
Core	.0573	0.0573[b] 0.0417		0.057	0.042	
Riser[c]	2.254	4.58		2.25	4.60	

[a] EBWR data obtained from reference 51 p. 138-139.

[b] Outer region contained two types of fuel elements.

[c] EBWR was also equipped with a common riser above the central and outer region risers having the following dimensions: length 3.5 ft., area 11.04 $ft.^2$, equivalent diameter 3.75 ft.

Table 2. Summary of flow investigations

run No.	form of power variation in Channel I	power density ratio (Channel I/ Channel II) initial	final	total power Channel II megawatts	length of run (sec)
1.1	steady	0.758	0.758	47.23	2.0
1.2	decreasing ramp	0.758	0.000	47.23	11.0
2.1	increasing ramp	0.000	0.600	47.23	5.0
3.1	steady	0.758	0.758	47.23	2.0
3.2	decreasing ramp	0.758	0.000	47.23	11.0
4.1	0.5 sec. step increase	0.000	0.050	51.96	9.0
4.2	0.5 sec. step increase	0.500	0.100	51.96	9.0
5.1	0.5 sec. step increase	0.000	0.100	51.96	9.0
5.2	0.5 sec. step increase	0.000	0.150	51.96	9.0
6.1	0.5 sec. step increase	0.000	0.010	51.96	14.0
	sinusoidal				
6.2	0.6 sec. period	0.950	1.050	51.96	4.0
6.3	0.8 sec. period	0.950	1.050	51.96	4.0
6.4	1.0 sec. period	0.950	1.050	51.96	4.0
6.5	1.2 sec. period	0.950	1.050	51.96	4.0
6.6	increasing ramp	1.000	2.800	51.96	14.5
	sinusoidal				
7.1	1.5 sec. period	0.950	1.050	51.96	5.2
7.2	1.8 sec. period	0.950	1.050	51.96	6.3
7.3	2.1 sec. period	0.950	1.050	51.96	7.3
7.4	2.4 sec. period	0.950	1.050	51.96	8.4

about 15 seconds to calculate the changes in the 22 node model that occurred during one second

A. Steady State and Ramp Results

Initial runs were made to determine the behavior of the model with constant heat generation rates and to look for possible regions of instability. Figure 10 shows an initial run. In all figures the exit velocity is the velocity the fluid would have as it exits from the riser if the mass flow were liquid and if the liquid were flowing through the inlet to the channel. In this run the initial heat generation rate in region I was 0.76 times that in region II and after two seconds the power in channel I was decreased. The initial void profile was assumed to be linear in the boiling region and constant after the flow left the boiling region. Several characteristics of the system can be observed from the results of this run. The following are of particular interest.

1. The flow oscillations into and out of the system are in general out of phase while the system is reaching equilibrium from the given flow conditions. This is to be expected. An increase (or decrease) in the average void constant of a channel will require a net decrease (or increase) in the mass flow rate into the system. Conservation of momentum in the channel will require the change in mass flow in and out of the system to be out of phase.

2. The large initial oscillations are the result of the

initial conditions selected. However, the system is self-damping and the flow is stabilized after about two seconds of operation.

3. The period of oscillation appears to be about 0.8 seconds. This is in general agreement with the power oscillations in the EBWR following a step change in reactivity, (64). This similarity could be fortuitous because the EBWR power involves a much more complicated feedback system than the one examined here.

4. The steady state circulation rate at this power level is 4.5 fps in region II and 4.9 fps in region I. For a corresponding power level in EBWR the average circulation rate is 4.5 fps (58b p.31). This indicates that the model is producing a reasonably steady-state solution of the flow rate.

Figure 10 also shows the behavior of the flow in channel I when the heat generation rate in the channel decreases linearly to zero and also when the power is increased linearly from zero. The flow again is stable into and out of the channel. The flow follows the general pattern that is expected.

The alternate curves shown in Figure 11 result from a simplification of the flow calculation procedure. The curve results from assuming that changes in pressure from the time rate of change of heat generation and the time rate of change of voids cancel each other and these terms are dropped from

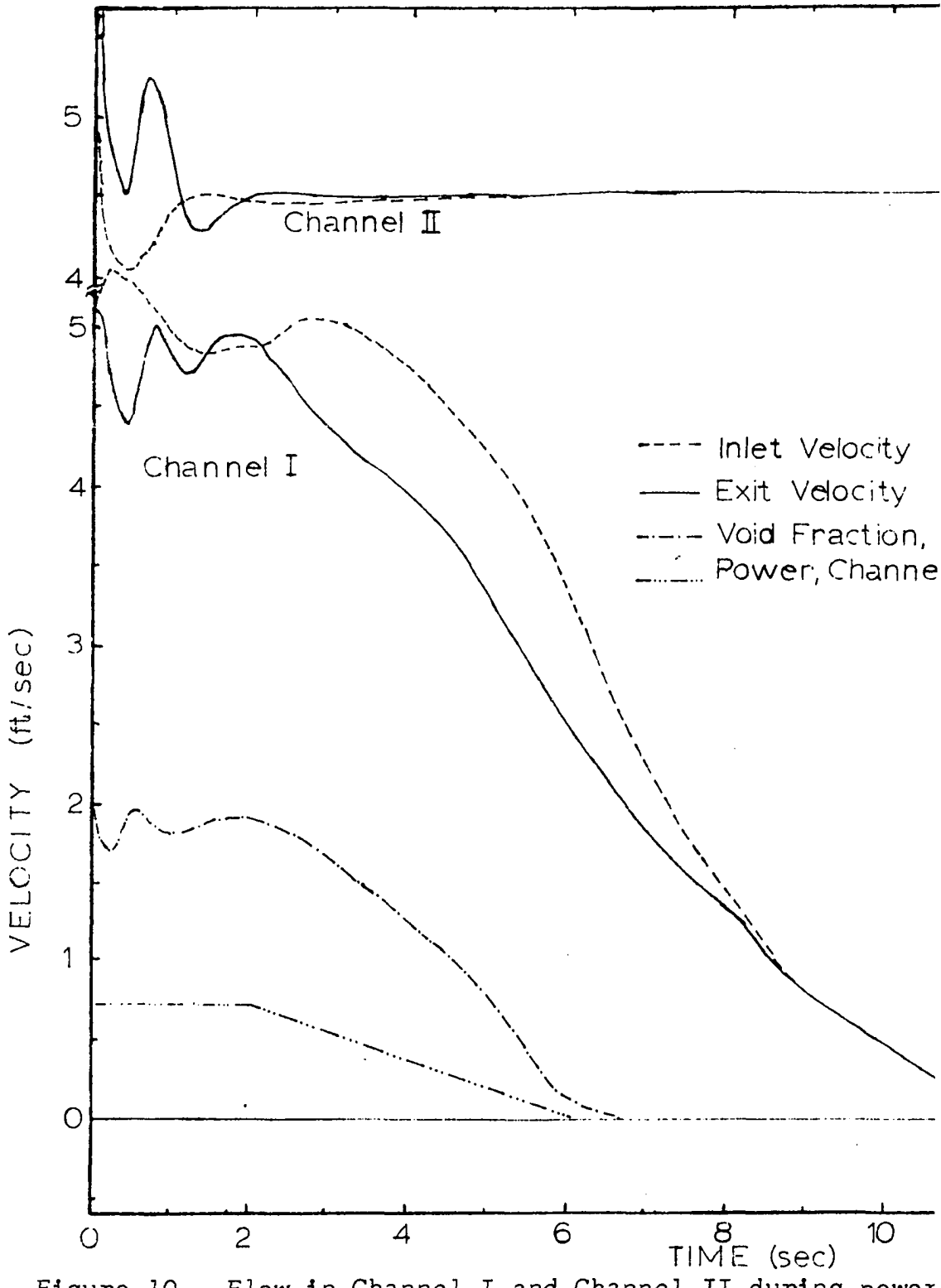

Figure 10. Flow in Channel I and Channel II during power

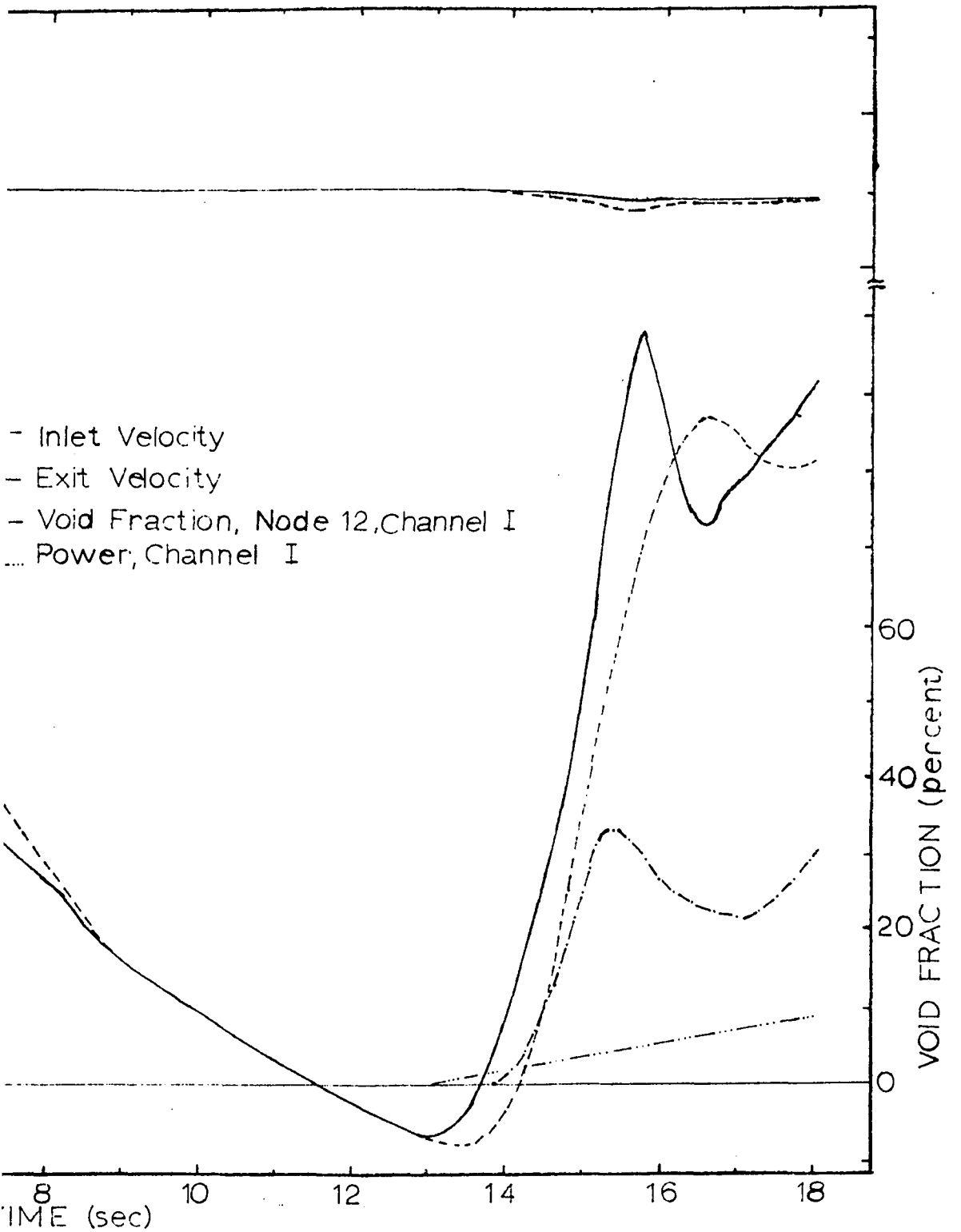

. II during power change in Channel I

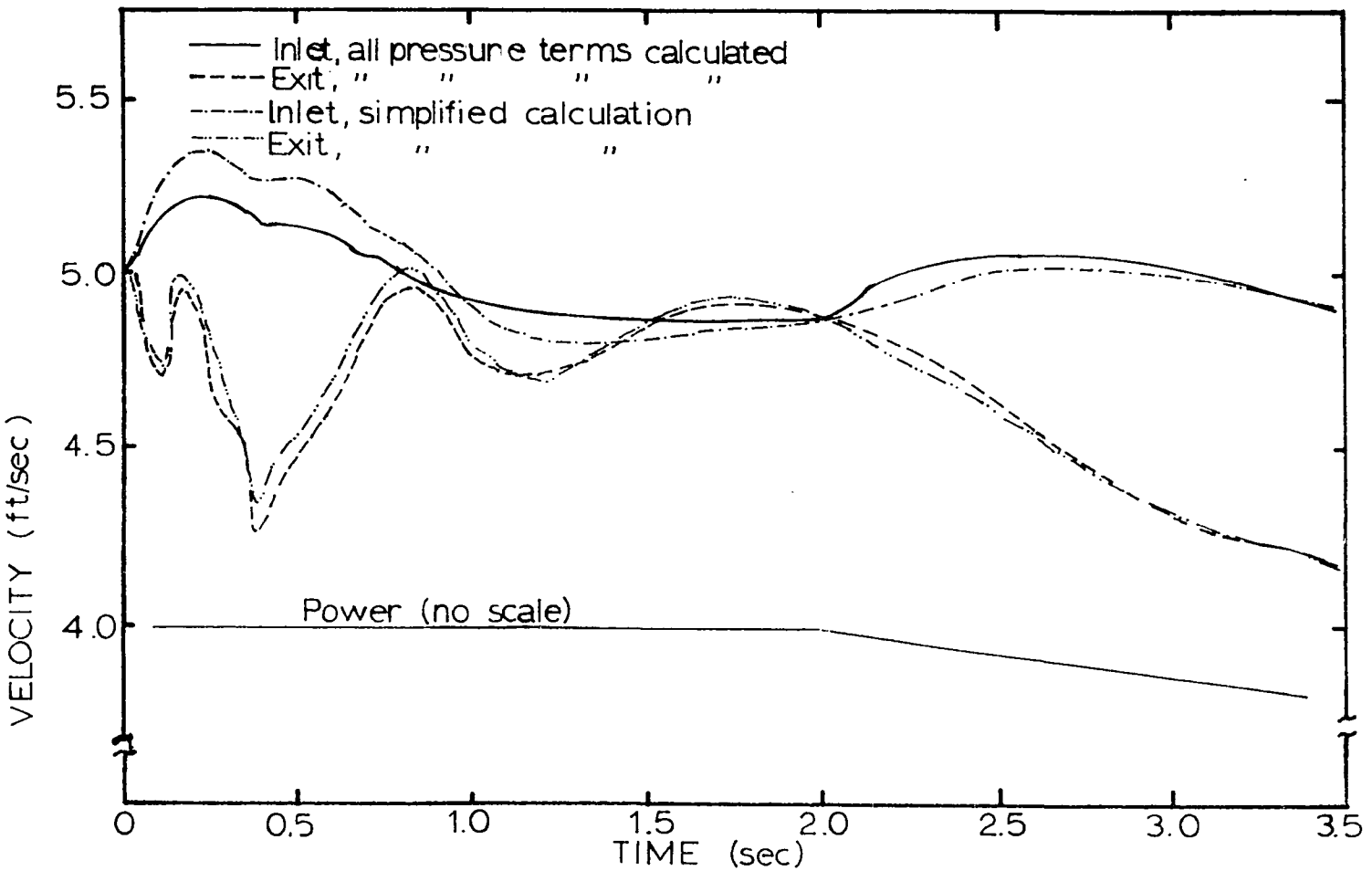

Figure 11. Comparison of Channel I flow when using different calculation procedures

the calculations. In the simplified curve the pressure drop across a channel consists of friction, spatial acceleration, gravity, and temporal acceleration terms where the temporal acceleration term is calculated assuming both phases have the same acceleration. It can be seen that the curves follow each other quite closely. The inclusion of the void and heat generation terms tends to dampen the oscillations in Figure 11 where the heat generation rate is constant, but in the region of decreasing heat generation rate, it can be seen that the inclusion of the heat generation term tends to accelerate the flow slightly more during the initial part of the change, but that both calculation procedures result in the approximate same flow pattern. This would indicate that the pressure drop due to these terms is very small. They were included in remaining calculations, but a savings in computational time could be obtained by omitting this part of the calculation procedure.

Ramp function

The behavior of the model at high power levels was investigated by imposing a ramp function on the power in channel I while the power in channel II remained constant. The results of this are shown in Figure 12. The first two seconds of flow are not plotted because faulty programming resulted in a poor set of initial conditions. After this time

the flow into and out of the channel remained relatively stable and showed a decreased flow rate as power increased. Some non-divergent flow oscillations were observed when the power in Channel I was between 1.8 and 2.2 times the power in Channel II. These oscillations had a period of about 1.0 second. The time for a bubble to travel from the center of the heated region to the channel exit was about 0.6 seconds for these flow conditions. The cause of this oscillation was not investigated in greater detail.

B. Flow Reversals

The curves shown in Figures 13 and 14 show the results of attempts to introduce conditions that would produce flow oscillations in Channel I while Channel II continued to operate at its existing power level. Initially the flow in Channel I was downward and there was no heat generation in this channel. Heat was introduced in Channel I in the form of a half second ramp followed by a steady heating rate. In all tests the average heating rate in Channel II was 65.5 kilowatt per liter of coolant and the heating rate in Channel I was made the indicated fraction of this heating rate. The same initial conditions were used in all tests.

The introduction of heat in Channel I produced a flow reversal characterized by an initial surge and a damped approach to a steady-state. The size of the initial surge

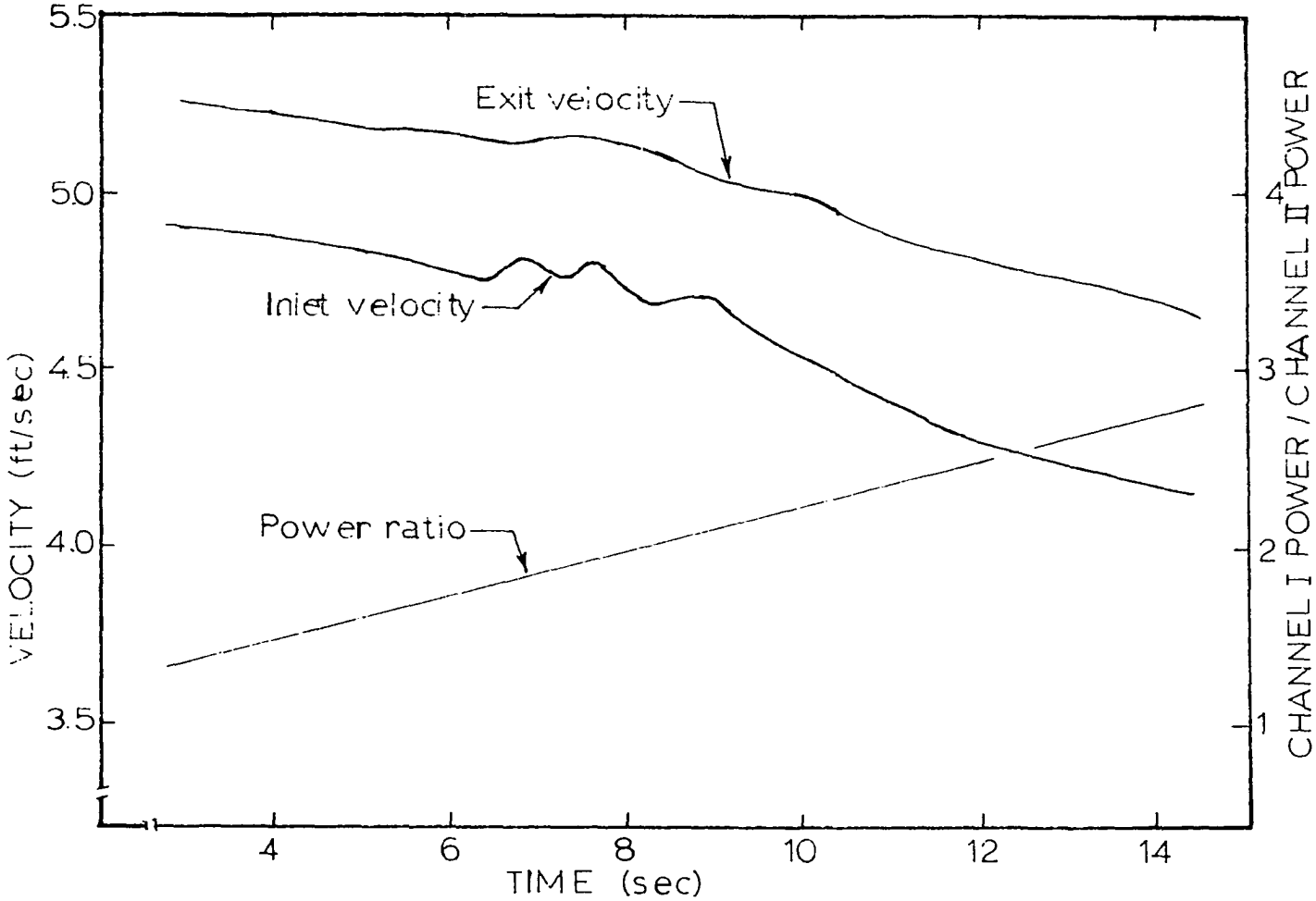

Figure 12. Channel I flow during ramp increase, run 6.6

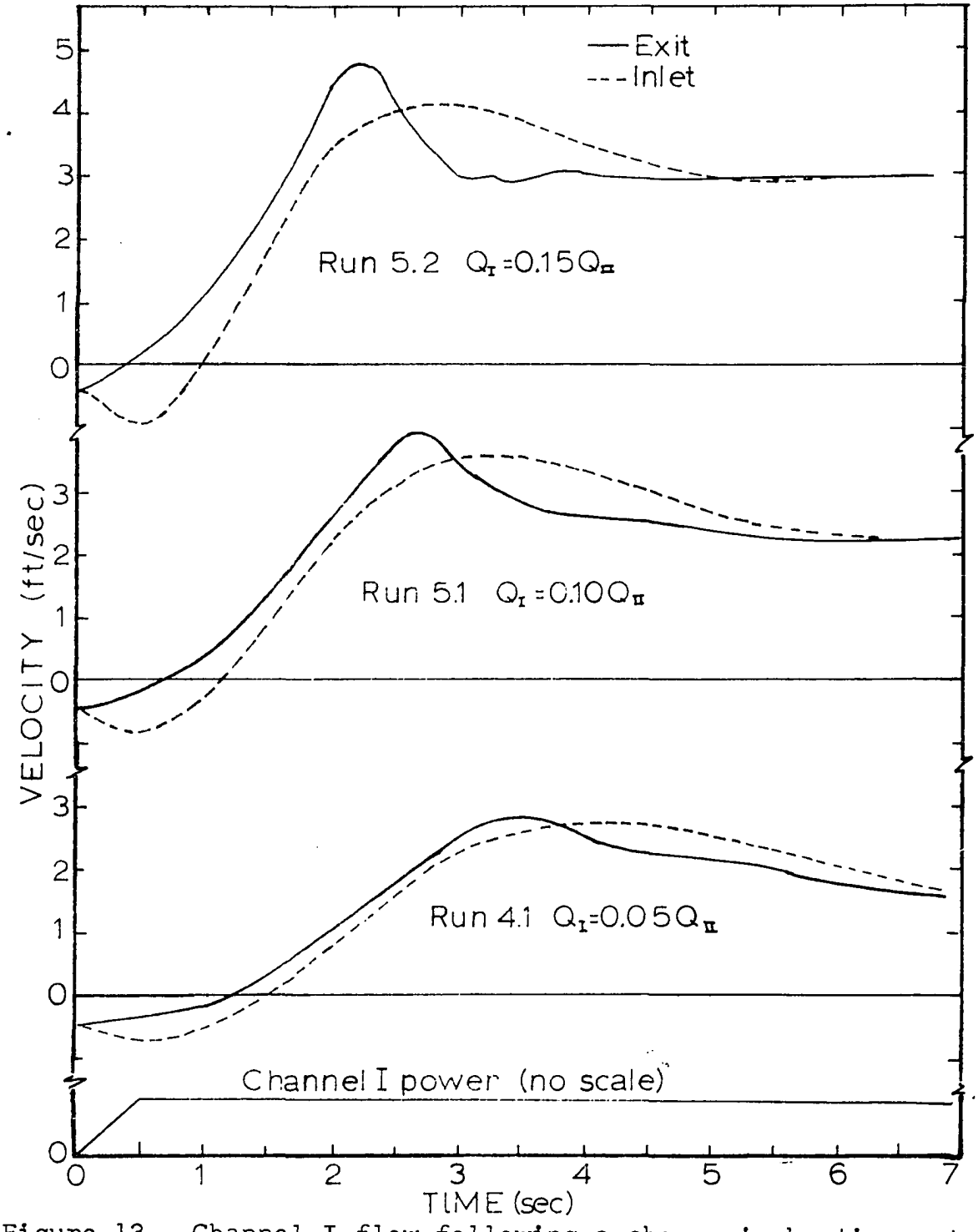

Figure 13. Channel I flow following a change in heating rate

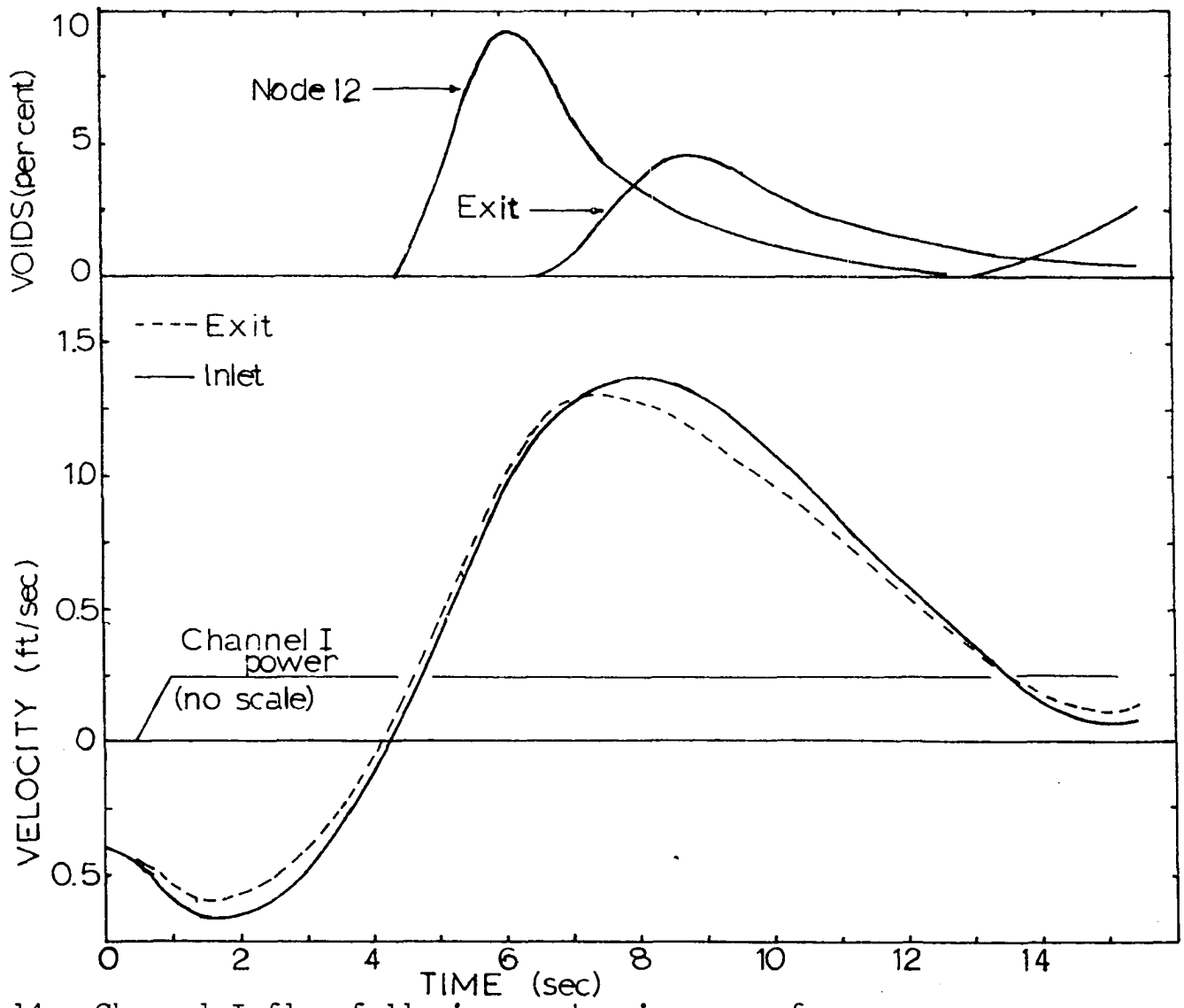

Figure 14. Channel I flow following a step increase from zero power
Channel I power = 1% Channel II power

increased with the size of the step increase in power, but the time for the flow to reach equilibrium decreased with the larger power steps. Figure 14 shows the flow pattern when the heating rate in Channel I is 1 percent of that in Channel II. The flow has not stabilized after 14 seconds when the computer program was stopped although the flow curves appear to be convergent. With this heating ratio all the voids were swept from the heated portion of the channel by the initial surge. The voids were not removed from the channel by the larger step increases in power.

These results indicate that any flow oscillations that might be developed in a channel having a low heating rate in parallel with a channel having a much larger heating rate would have a very low frequency and probably would be convergent without power feedback from a reactor.

The effect of the riser during a flow reversal may be analyzed by dividing the flow reversal into three phases: 1. The initial phase where a voided region of "slug" is formed and the flow reversal starts, 2. The intermediate phase where the slug is swept through the channel, and 3. A damping phase where the flow reaches a new steady-state value.

The initial phase is characterized by the slug formation and the flow reversal. During this interval the average density in the channel is reduced by the slug and the

resultant buoyant force causes the flow to begin its upward acceleration. The riser reduces the magnitude of this initial acceleration two ways: 1. The average reduction in density in the column which produces the driving force for a flow change is limited by the liquid region above the slug. The percentage of voids in the slug may be much greater than that found in the channel during steady-state operation, but the average percentage of voids in the channel is not as great due to the dense region above the slug. 2. The mass that must be accelerated by the buoyant force is increased due to the unvoided region in the riser. Therefore, the effect of the riser during the first phase of the flow reversal is to reduce the acceleration. The void distribution for the channel during phase one can be characterized by the curve shown at 1.18 seconds in Figure 15.

During the second phase of the reversal the slug is carried into the riser region. If the riser region were not present the slug would pass out of the channel and the newly formed buoyancy force would be lost. The riser allows the acceleration to continue, but the effect of the slug is minimized because it occupies only a portion of the channel and the overall change in density is not as great as the change in slug density.

During the final phase the slug leaves the channel and the flow reverts to a steady-state velocity. The slug is followed

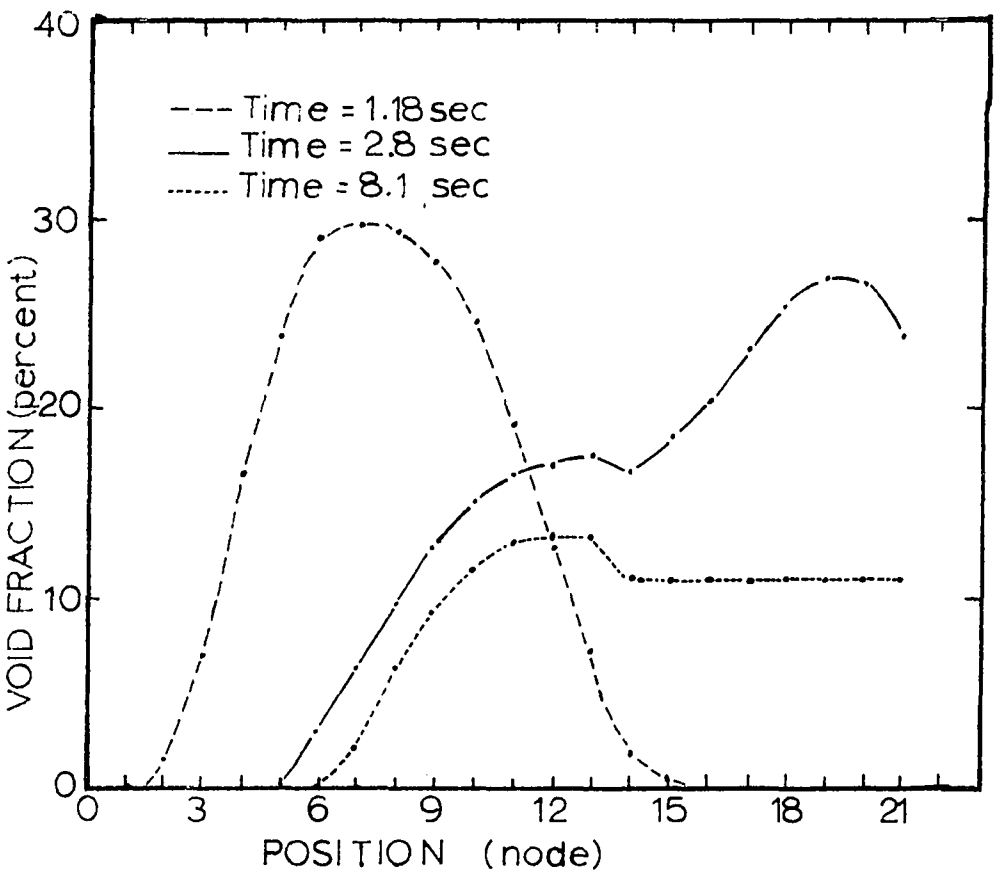

Figure 15. Void distribution in Channel I during run 5.2

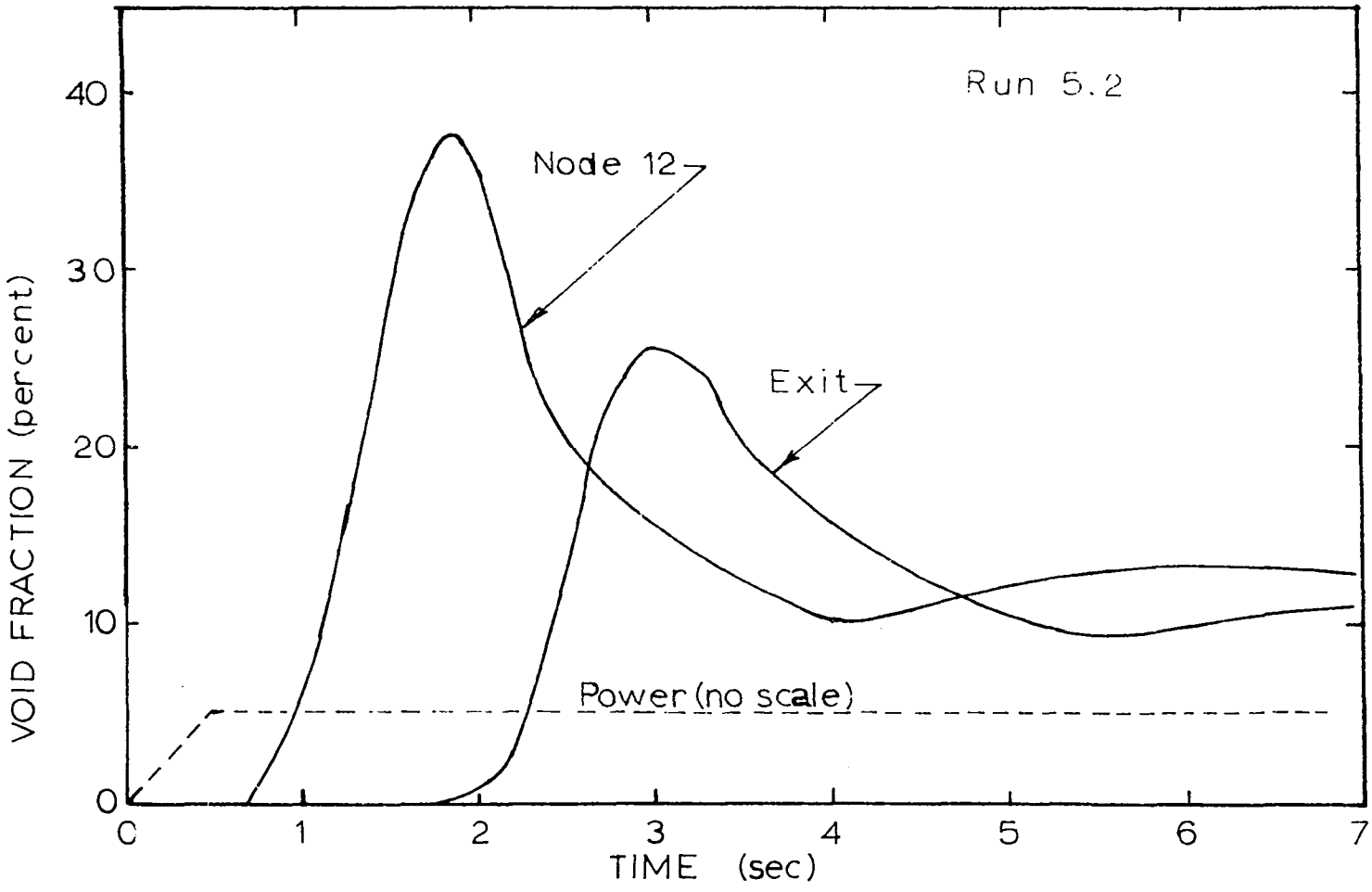

Figure 16. Time variation of void fraction following a power increase

by a region of decreasing voids as the slug leaves and the riser tends to smooth out any abrupt change in buoyancy by averaging the density in the column. The steady-state void distribution is described by the final curve in Figure 15. The decrease in void fraction at node 15 in the final curve is a result of the increase in flow area at this node.

The sudden damping of the exit velocity in the 0.15 Q_2 curve in Figure 13 which occurs approximately 3 seconds after the excursion began can be explained by the arrival of the slug at the channel exit at this time. The plotted velocity is the velocity the mass would have if liquid only were flowing. Immediately following the arrival of the slug the flow appears to be damped due to the increased mass flowing per unit area. The actual liquid velocity would continue to decrease, but the increasing mass flow per unit area causes the mass flow rate to remain essentially constant and give the appearance of a very sudden damping.

C. Power Oscillations

The response of the two-phase flow of the model to power oscillations was determined by sinusoidally oscillating the power in Channel I while the power in Channel II remained constant. During this part of the investigation the steady-state component of the power in Channel I was equal to the power in Channel II and the sinusoidal component of the power

in Channel I at each node had a maximum magnitude equal to 5 percent of the steady-state power at that node. The system was started with approximately steady-state flow conditions and the effects on flow parameters were observed as the power was oscillated. The power was oscillated at periods from 0.6 to 2.4 seconds. The results of this investigation are presented in Table 3 and results are shown graphically in Figures 17, 18, 19 and 20. These figures indicate that the maximum exit velocity response to the power oscillation appears to be at a period of about 1.5 seconds or 4.19 radians per second.

Table 3. Results of 5% power oscillation in Channel I

run	period (sec.)	velocity (fps)[a] inlet	exit	void fraction center	exit
6.2	0.6	0.35	0.18	0.019	0.008
6.3	0.8	0.35	0.18	0.026	0.016
6.4	1.0	0.36	0.41	0.032	0.023
6.5	1.2	0.37	0.58	0.035	0.026
7.1	1.5	0.35	0.61	0.036	0.028
7.2	1.8	0.32	0.59	0.035	0.029
7.3	2.1	0.29	0.52	0.034	0.029
7.4	2.4	0.25	0.46	0.032	0.028

[a]Exit velocities are the velocity the fluid would have if all the mass were liquid and the liquid were flowing in a channel having the same area as the inlet to the channel.

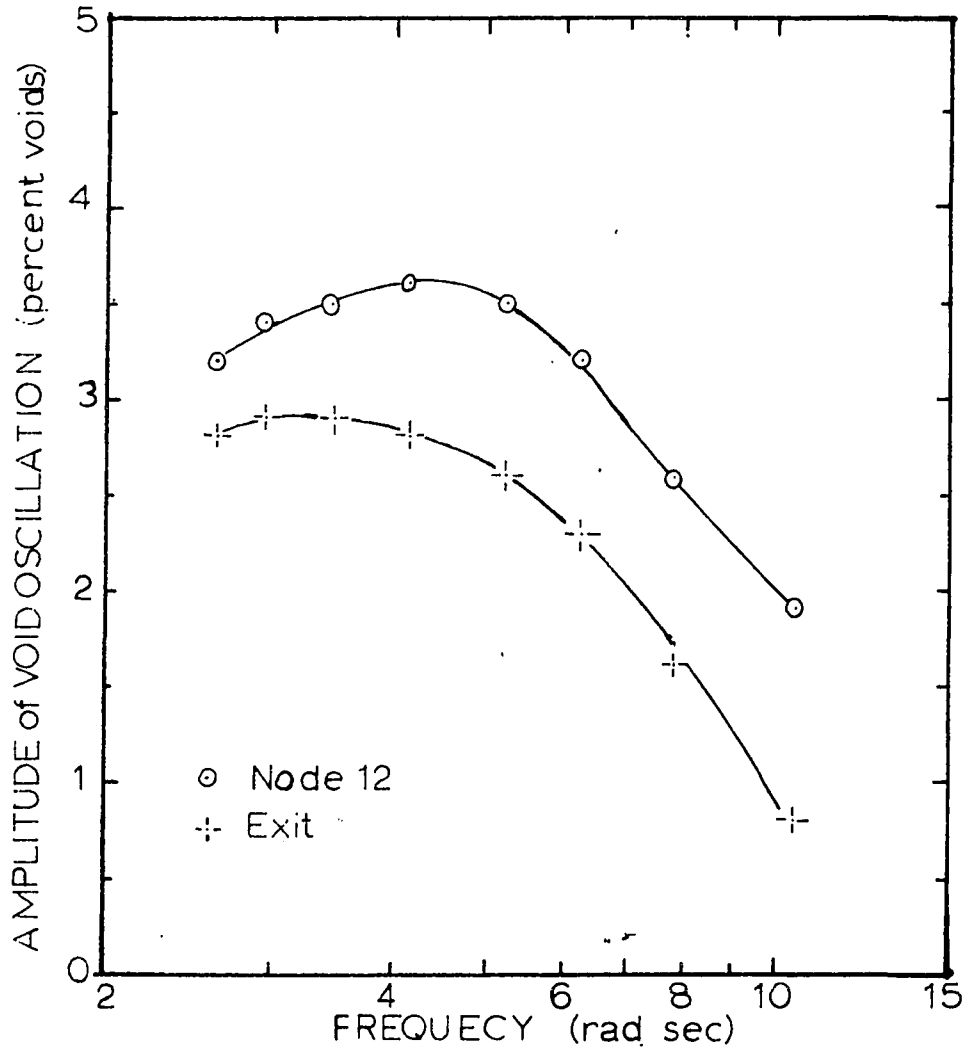

Figure 17. Response of Channel I void fraction to 5% power oscillation

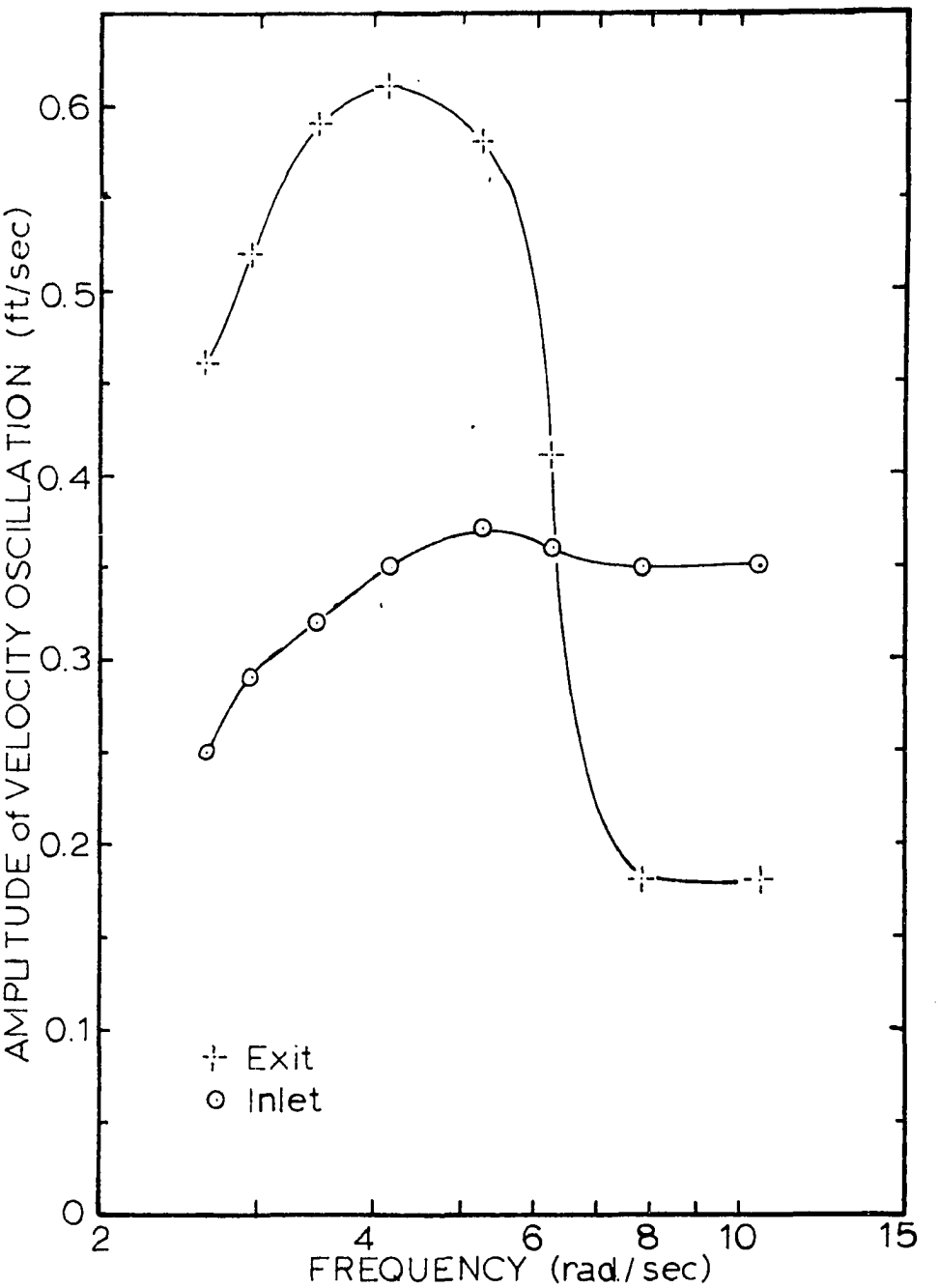

Figure 18. Response of Channel I flow to 5% power oscillations

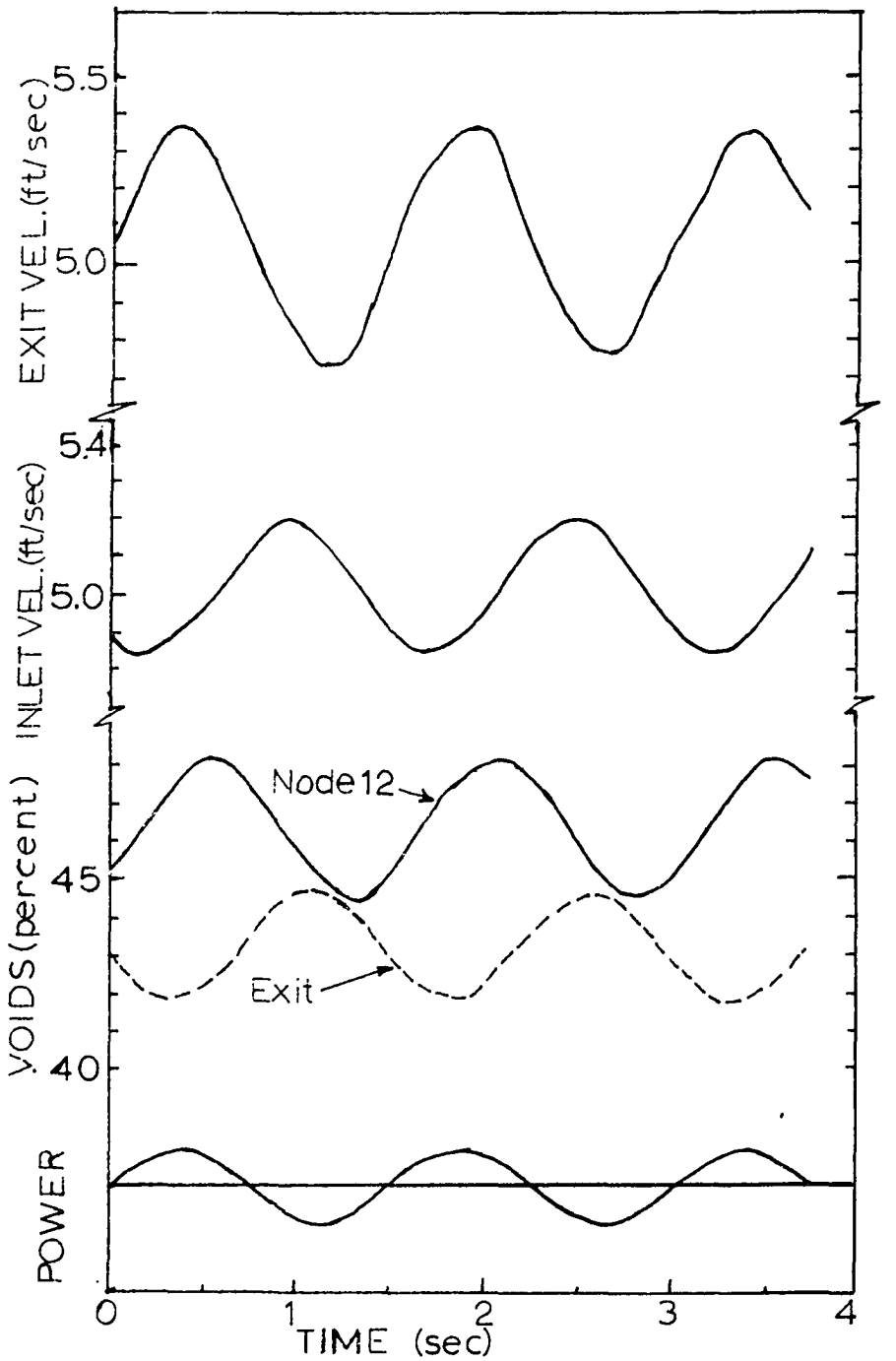

Figure 19. Response of Channel I to 5% power oscillations with 1.5 sec. period, run 7.1

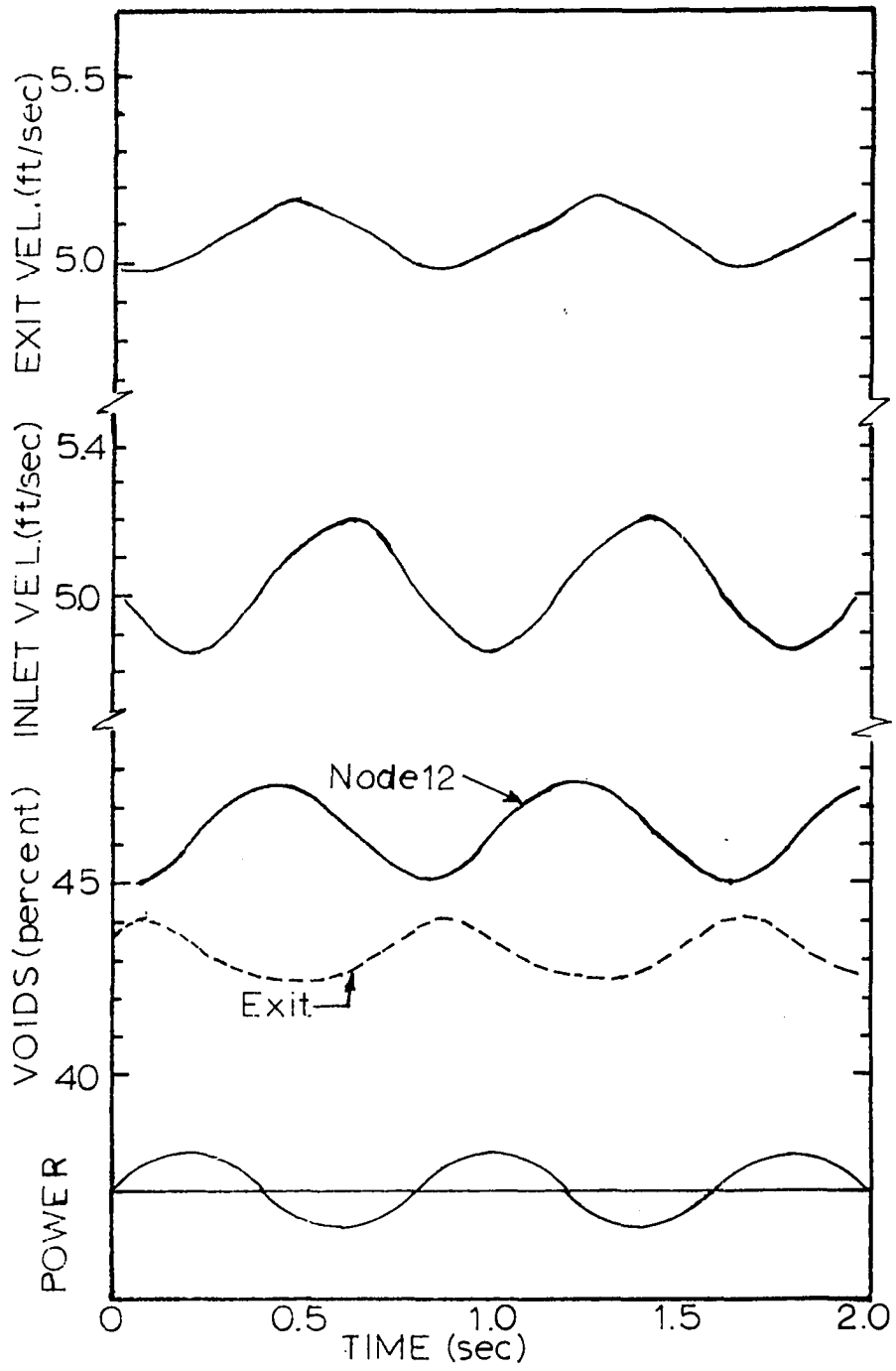

Figure 20. Response of Channel I to 5% power oscillations with 0.8 sec. period, run 6.3

The response of the model to power oscillations is not in agreement with the computed natural frequency of the system. Such calculations neglecting the mass of the fluid in the lower plenum indicate that the columns would oscillate with a period of about 3.5 seconds.

The critical period of the system can be determined by analyzing the movement of a voided region up a channel. As a region of high voids goes up the channel this region will contribute to a velocity change by two methods. First, the region of high voids will increase the buoyancy of the channel and this will tend to increase the upward acceleration of the components. Second, the voided region, as it exits from the channel, will increase the spatial acceleration of the liquid and the pressure drop due to this effect will decellerate the fluid.

Another factor which affects the acceleration of the fluid is the change in heating rate. An increase in heating rate increases the void generation rate and this will accelerate the fluid above the boiling region and decellerate the fluid below this region.

The acceleration due to a change in void generation rate can be combined with the acceleration due to spatial acceleration to predict the critical frequency at which the amplitude of the flow oscillation is at a maximum. The spatial acceleration pressure drop causes all nodes in a

channel to be accelerated at an approximately uniform rate. Thus, when a region of low voids is exiting from a riser the spatial acceleration pressure drop is low and the entire channel is being accelerated upward due to this effect. If, at the same time, the void fraction is increasing at the nodes in the heated region, the nodes above this region will be accelerated upward and those nodes below this region will be accelerated downward. The result under these conditions is reinforcement of the upward acceleration at the nodes above the boiling region.

The same reasoning may be applied to reinforce the deceleration of the nodes above the heated region when a region of high voids is exiting from the channel and the void fraction in the heated region is decreasing due to a reduction in heat generation rate.

In Figure 19 it is noted that the exit void fraction and the heat generation rate are nearly out of phase. This means that the accelerations due to spatial acceleration pressure drop and due to a change in void generation are reinforcing each other in the nodes above the heated section and that the exit liquid velocity should have its maximum amplitude. At this frequency the exit flow velocity exhibited the maximum change that was observed at any of the imposed frequencies.

A damping effect on the exit velocity is observed when the void wave arrives at the exit approximately in phase with

the power. This is shown in Figure 20.

This suggests that the maximum flow disturbance or response to power oscillations will occur when the time for the slug to travel to the end of the channel is one half the period of the power oscillation, or

$$\tau = 2\Delta T \qquad 63$$

Where τ is the period, and ΔT is the time for the void wave to move from its generation point to the exit from the channel.

In the model the calculated time for a bubble to travel from the center of the boiling core to its exit from the channel under these conditions was 0.74 seconds, thus predicting a critical period of 1.48 seconds and a frequency of 4.24 radians per second.

This period is not in agreement with the 0.628 second period observed in EBWR at 600 psi and 50 MW power (64). However, EBWR was not equipped with risers when the frequency response curves were obtained. The spatial acceleration pressure drop would occur when the voids left the one foot extension on the fuel elements. The EBWR inlet velocities at this power were approximately 4.25 fps and the exit voids were 35 percent (64, p. 44). Using a slip ratio of 1.5 this gives a transient time from the center of the core to the exit from the core of about 0.32 seconds, and the correlation given in Equation 63 predicts a period of 0.64 seconds.

It would be presumptious to say that the feedback in the EBWR was due completely to the hydraulic effect discussed above. However, this could have been a cause. It must be realized that the feedback in EBWR is more complicated and involves all the nuclear characteristics that have not been considered in the development of this model.

Other observers (10) have noted that the period of oscillation was approximately equal to the time for the liquid to pass through the channel.

D. Coupling Between the Risers

The effect of changes in Region I on the flow in Region II are summarized in Table 4. From this it can be seen that the coupling effect between the two channels was small and that with this geometry Channel I acted almost as a single channel with a constant pressure drop. In this model the flow areas of Channel I, Channel II, and the downcomer at the lower plenum are 2.0, 7.0, and 14.0 square feet, respectively. A perturbation in the smaller channel would not be expected to have an equivalent effect on the larger channels.

E. Circulation Rates

Figure 21 is a comparison of the circulation rates in the model to those observed in EBWR. The circulation rates are in good agreement except at low power. The model circulation rates at low powers were obtained from the circulation rate of Channel I when its power was reduced and Channel II

Table 4. Coupling effect between channels

run no.	type of flow disturbance Channel I	power ratio $\frac{\text{Channel I}}{\text{Channel II}}$ initial	power ratio $\frac{\text{Channel I}}{\text{Channel II}}$ final	inlet velocities (fps) Channel I min.	Channel I max.	Channel I ΔV	Channel II min.	Channel II max.	Channel II ΔV	disturbance ratio $\frac{\Delta V_{II}}{\Delta V_{I}}$
6.1	step increase	0.00	0.01	-0.66	1.37	2.03	4.50	4.47	.03	.0147
4.1	step increase	0.00	0.05	-0.70	2.77	3.47	4.43	4.50	.07	.0202
4.2	step increase	0.05	0.10	1.26	2.55	1.29	4.48	4.45	.03	.0232
5.1	step increase	0.00	0.10	-0.83	3.56	4.39	4.49	4.38	.11	.0250
5.2	step increase	0.00	0.15	-.92	4.13	5.05	4.52	4.34	.18	.0358
3.2	ramp decrease	0.76	0.00	-.21[a]	5.05	5.26	4.52	4.45	.07	.0133
	sinusoidal									
6.2	0.6 sec. per.	0.95	1.05	4.86	5.19	0.33	4.43	4.47	.04	.1210
6.4	1.0 sec. per.	0.95	1.05	4.85	5.21	0.36	4.42	4.48	.06	.1670
7.1	1.5 sec. per.	0.95	1.05	4.85	5.20	0.35	4.43	4.47	.04	.1140
7.3	2.1 sec. per.	0.95	1.05	4.88	5.17	0.29	4.43	4.46	.03	.1030

[a]Program stopped before velocity had reached equilibrium.

continued to operate at a higher power. Therefore these circulation rates are not the exact rate the system would have if the power were the same in all channels, but they do indicate a general agreement between the model and EBWR.

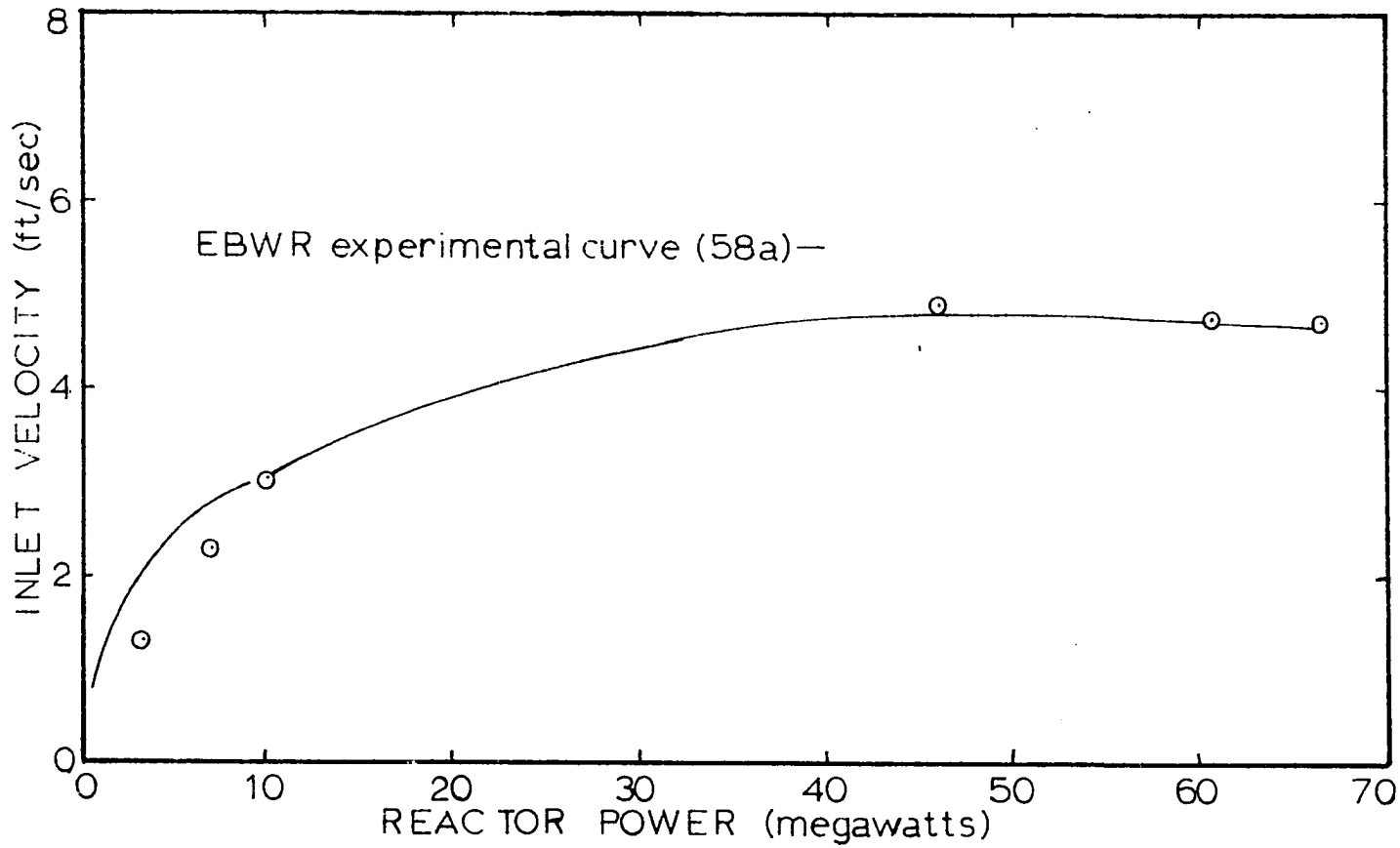

Figure 21. Comparison of model and EBWR circulation rates

VIII. CONCLUSIONS

The major conclusions to be drawn from the investigation are as follows:

1. The model showed no divergent or sustained oscillations during any part of the testing.

2. The maximum response of the model to power oscillations occured when the period of the power oscillation was twice the time required for a bubble to exit from the channel.

3. The model, when compared with EBWR experimental data, predicted recirculation rates within 5 percent at reasonable reactor power.

4. The solution of the flow equations in terms of liquid velocity, vapor velocity, and void fraction permits an insight into the actual events taking place during a distrubance that is not obtained from transfer functions or mass flow calculations.

5. The effect of a change in heat generation rate and a change in void fraction generation rate on system acceleration is small during a flow perturbation.

6. A change in flow in the smaller channel had a small effect on the flow in the larger channel.

7. The analysis presented in this thesis successfully predicted the steady-state behavior of the model analyzed and, although no data were available for comparison, gave reasonable values for the behavior of the system following power

changes. The EBWR, with its more complex feedback system, showed no power oscillations in its operation and this analysis showed that it is hydraulically stable.

IX. SUGGESTIONS FOR FURTHER WORK

This thesis presents a method of analyzing steady and non-steady two-phase flow in two parallel channels in a boiling loop. This analysis could be used to examine an almost unlimited number of two-phase flow problems. Improvements in the analysis could be made with a combination of theoretical and experimental work. Some suggestions for further work are listed below.

1. Improvement of computer program. Specific items that might be improved are
   a. Include subcooled boiling and carryunder in calculations.
   b. Expand the pressure drop calculations to include more accurate orifice and form pressure drop terms.
   c. Examine various methods to reduce calculation time.
   d. Introduce a void-power feedback.
   e. Add additional risers.

2. Experimental program. The mathematical model should be checked with an experimental program. This would add considerable insight into the phenomenon occurring. Other related experimental programs could include
   a. Determination of bubble velocities when flow is reversed.

b. Effect of oscillations on the behavior of the components of two-phase flow.

3. Further experiments using the same computer program. The effects of numerous parameters on flow stability could be investigated with the existing computer program. Different pressures, geometries, and steam release rates are a few of the parameters that could be investigated.

X. ACKNOWLEDGEMENTS

To Dr. Glenn Murphy, without whose inspiring guidance and constant encouragement this work would have never been done, the author here expresses his most sincere gratitude.

The author also acknowledges the assistance of the Iowa State University Computational Center in providing computer time for unsponsored research and the assistance of Dr. Clair Maple for timely discussions on the numerical solution of the differential equations.

The author would also like to express his gratitude to his wife for her encouragement and sacrifice which have made the attainment of this goal possible.

XI. NOMENCLATURE

Primary English Letter Symbols

A	area, sq. ft.
d	diameter, ft.
f	friction factor
g	acceleration of gravity, ft./sec.^{2}
G	mass flow rate per unit area, lb.-sec./ft.^{3}
h	enthalpy, Btu/lb.
h_{fg}	heat of vaporization, Btu/lb.
i	node designation
j	channel designation
L	length, ft.
P	pressure, lb./lb.-ft.^{2}
Q	heat generation rate, Btu/ft.^{3} -sec.
R	friction factor multiplier
T	time, sec.
U	reduced liquid velocity- V(1-Ø), ft./sec.
U"	reduced vapor velocity-V.Ø, ft./sec.
v	specific volume, ft.^{3}/lb.
v_{fg}	specific volume of vaporization, Btu/lb.
V	vapor velocity, ft./sec.
V"	vapor velocity, ft./sec.
W	mixture velocity U+U", ft./sec.
x	steam quality
Z	node before increase in flow area

Primary Greek Letter Symbols

Δ	finite increment difference
ρ	liquid density, lb. sec.^{2}/ ft.^{2}
ρ''	vapor density, lb. sec.^{2}/ ft.^{4}
σ	surface tension, lb./ft.
μ	liquid viscosity, lb.-sec./ ft.^{2}
ϕ	ratio of channel area occupied by vapor to total channel area

Subscripts

i	node designation
j	channel designation
k	time designation
v	vapor
f	liquid
fg	liquid to vapor transformation
x	position, ft.

XII. LITERATURE CITED

1. Anderson, R.P. The calculation of steady state hydraulics and stability studies at ANL of natural circulation boiling water reactors. Advanced course on the dynamic behavior of boiling water reactors, Kjeller, Norway, 1962. U.S. Atomic Energy Commission Report KR-35, Vol. 1 (Norway, Institutt for Atomenergi, Kjeller) IX. 1-IX. 54. 1963.

2. _____, Bryant, L.T., Carter, J.C., and Marchaterre, J.F. Transient analysis of two phase natural circulation systems. U.S. Atomic Energy Commission Report ANL-6653 (Argonne National Laboratory, Argonne, Illinois). 1962.

3. _____ and Lottes, P.A. Boiling stability. Progress in Nuclear Energy, Ser. IV, Vol. 4:3-28. New York, N.Y., Pergamon Press. 1961.

4. Andronow, A.A. and Chaikin, C.E. Theory of oscillations. Princeton, N.J., Princeton University Press. 1949.

5. Bankoff, S.G. A variable density single-fluid model for two-phase flow. American Society of Mechanical Engineers Transactions. Ser. C, 82: 265-272. 1960.

6. Beckjord, E.S. Dynamic analysis of natural circulation boiling water power reactors. U.S. Atomic Energy Commission Report ANL-5799 (Argonne National Laboratory, Argonne, Illinois). 1958.

7. _____. Instability problems. Proceedings of the 1960 Idaho conference on reactor kinetics. U.S. Atomic Energy Commission Report IDO-16791 230-234 (Idaho Operations Office, AEC, Idaho Falls, Idaho). 1960.

8. _____. The stability of two-phase flow loops and response to ships motion. U.S. Atomic Energy Commission Report GEAP-3493, Rev. 1 (General Electric Atomic Power Department, San Jose, Cal.). 1960.

9. _____ and Harker, W.H. Hercules I, the steady-state calculation of vertical two-phase flow. U.S. Atomic Energy Commission Report GEAP-3261 (General Electric Atomic Power Department, San Jose, Cal.). 1959.

10. _____ and Levy, S. Hydraulic instability in a natural circulation loop with net steam generation at 1000 psia. Paper 60HT27. American Society of Mechanical Engineers. 1960.

11. Behringer, P. Steiggeschwindigkeit von dampfblasen in kesselrohren. Verein Deutscher Ingenieure Forschungsheft 365: 4-12. 1934.

12. Bick, J.H. A new method for determining the stability of two-phase flow in parallel heated channels with application to nuclear reactors. U.S. Atomic Energy Commission Report NAA-SR-4927 (Atomics International, Canoga Park, Cal.). 1960.

13. Birkhoff, G. Hydrodynamics, a study in logic, fact, and similitude. 2nd ed. Princeton, N.J., Princeton University Press. 1960.

14. Blubaugh, A.L., and Quandt, E.R. Analysis and measurement of flow oscillations. U.S. Atomic Energy Commission Report WAPD-AD-TH-538 (Westinghouse Electric Corp., Atomic Power Division, Pittsburgh, Pa.). 1962.

15. Bowring, R.W. The calculation of subcooled voids. Advanced course on the dynamic behavior of boiling water reactors, Kjeller, Norway, 1962. U.S. Atomic Energy Commission Report KR-35, Vol. 1 (Norway, Institutt for Atomenergi, Kjeller) VIII.1 VIII.18. 1963.

16. Chernick, J. Discussion of two types of reactor instabilities. Proceedings of the 1960 Idaho conference on reactor kinetics. 246-250. U.S. Atomic Energy Commission Report IDO-16791 (Idaho Operations Office, AEC, Idaho Falls, Idaho). 1960.

17. Christensen, H. Introductory lecture. Sec. 1. Advanced course on the dynamic behavior of boiling water reactors, Kjeller, Norway, 1962. U.S. Atomic Energy Commission Report KR-35 Vol. 1 (Norway, Institutt for Atomenergi, Kjeller) I.1-I.19. 1963.

18. Cook, W.H. Boiling density in vertical rectangular multichannel sections with natural circulation. U.S. Atomic Energy Commission Report ANL-5621 (Argonne National Laboratory, Argonne, Illinois). 1956.

19. DeShong, J.A. Upping EBWR's power. Nucleonics 16, No. 6:68-72. June 1958.

20. _____ and Lipinski, W.C. Analysis of experimental power reactivity feedback functions for a natural circulation boiling water reactor. U.S. Atomic Energy Commission Report ANL-5850 (Argonne National Laboratory, Argonne, Illinois). 1958.

21. Dietrich, J.R. and Layman, D.C. Transient and steady state characteristics of a boiling reactor. The BORAX experiments, 1953. U.S. Atomic Energy Commission Report ANL-5211 (Argonne National Laboratory, Argonne, Illinois). 1954.

22. Fleck, J.A. The dynamic behavior of boiling water reactors. Journal of Nuclear Energy, Part A: Reactor Science 11:114-130. Feb. 1960.

23. _____. A model for hydraulic instability. Proceedings of the 1960 Idaho conference on reactor kinetics. U.S. Atomic Energy Commission Report IDO-16791 242-246 (Idaho Operations Office, AEC, Idaho Falls, Idaho). 1960.

24. Foglia, J.J. Boiling water void distribution and slip ratios in heated channels. U.S. Atomic Energy Commission Report BMI-1517 (Battelle Memorial Institute, Columbus, Ohio). 1961.

25. Forster, H.K. and Zuber, N. Dynamics of vapor bubbles and boiling heat transfer. American Institute of Chemical Engineers Journal 1:531-535. 1955.

26. Galson, A.E. Steam slip and burnout in bulk boiling systems. U.S. Atomic Energy Commission Report GEAP-1076 (General Electric Atomic Power Department, San Jose, Cal.). 1957.

27. Garlid, K., Amundson, N.R., and Isbin, H.S. A theoretical study of the transient operation and stability of two-phase natural circulation loops. U.S. Atomic Energy Commission Report ANL-6381 (Argonne National Laboratory, Argonne, Illinois). 1961.

28. George, W.D. The transient behavior of a two-phase natural circulation loop. Unpublished M.S. thesis. Austin, Texas, Library, University of Texas. 1960.

29. Hammond, P.H. Feedback theory and its applications. New York, N.Y., The Macmillan Co. 1958.

30. Haywood, R.W., Knights, G.A., Middleton, M.A., and Thom, J.R.S. Experimental study of the flow conditions and pressure drop of steam-water mixtures at high pressures in heated and unheated tubes. Institution of Mechanical Engineers Proceedings 175:669-948. 1961.

31. Hoglund, B.M., Epperson, T.R., and Weatherhead, R.J. Two-phase pressure drop for natural circulation in vertical rectangular channels. U.S. Atomic Energy Commission Report ANL-5760 (Argonne National Laboratory, Argonne, Illinois). 1959.

32. Isben, H.S., Sher, N.C., and Eddy, K.C. Void fractions in two-phase steam water flow. American Institute of Chemical Engineers Journal 3:136-142. March 1957.

33. Johnson, R.L. Kinetics, stability and control. A selected bibliography. U.S. Atomic Energy Commission Report NAA-SR-7786 (Atomics International, Canoga Park, Cal.). 1963.

34. Jones, A.B. Hydrodynamic stability of a boiling channel. U.S. Atomic Energy Commission Report KAPL-2170 (Knolls Atomic Power Laboratory, Schenectady, N.Y.). 1961.

35. _____ and Dight, D.G. Hydrodynamic stability of a boiling channel, Part 2. U.S. Atomic Energy Commission Report KAPL-2208 (Knolls Atomic Power Laboratory, Schenectady, N.Y.). 1962.

36. Kholodovskiy, G.E. Generalization of experimental data on the circulation of water in steam boilers. Heat power engineering, Part 1. Translation of Teploenergatika, Vypusk 1. Isdatel'stvo Akademii Nauk S.S.S.R., Moskva, 1959. U.S. Atomic Energy Commission Translation AEC-tr-4496 1-36 (Technical Information Service Extension, AEC). 1961.

37. Kirchenmayer, A. Dynamics of boiling water reactors. Advanced course on the dynamic behavior of boiling water reactors, Kjeller, Norway, 1962. U.S. Atomic Energy Commission Report KR-35, Vol. 2 II.1-II.44 (Norway, Institutt for Atomenergi, Kjeller). 1963.

38. _____. On the kinetics of boiling water reactors. Journal of Nuclear Energy, Part A: Reactor Science 12: 155-161. 1960.

39. Kjelland-Fosterud, E. Two-phase flow. Sec. V. Advanced course on the dynamic behavior of boiling water reactors, Kjeller, Norway, 1962. U.S. Atomic Energy Commission Report KR-35, Vol. 1 V.1-V16 (Norway, Institutt for Atomenergi, Kjeller). 1963.

40. Kolba, V.M. EBWR test reports. U.S. Atomic Energy Commission Report ANL-6229 (Argonne National Laboratory, Argonne, Illinois). 1960.

41. Kornbichler, H. The static hydraulic stability of boiling water reactors. Translation of Diestatische hydra lische stabilitat von siedewasserreaktoren. Atomkernenergie 5: 1960. U.S. Atomic Energy Commission Translation AEC-tr-4995 397-400 (Technical Information Service Extension, AEC) 1962.

42. Kramer, A.W. Boiling water reactors. Reading, Mass., Addison-Wesley Publishing Co. 1958.

43. Kutateladze, S.S. Heat transfer in condensation and boiling. Translation of Teploperedacha pri kondensatsii i kipenii. Vtoroe izdanie, dopolnenoe i pererabotannoe. Gosudarstvennoe izdatel' stvo Nauchno-Tekhnicheskoi Literatury po Mashinovedeniiy, Moskva/Leningrad. 1952. U.S. Atomic Energy Commission Translation AEC-tr-3770 (Technical Information Service Extension, AEC). 1959.

44. Ledinegg, M. Unstabilitat der Stromung bei naturlichem und Zwangsumlauf. Die Warme, 61, 891-898. 1938.

45. Levy, S. Steam slip-theoretical prediction from momentum model. American Society of Mechanical Engineers Transactions. Ser. C. 82:113-124. 1960.

46. Lockhart, R.W. and Martinelli, R.C. Proposed correlation of data for isothermal two-phase, two component flow in pipes. Chemical Engineering Progress 45:39-48. 1949.

47. Longly, H.J. Methods of differencing in Eulerian hydrodynamics. U.S. Atomic Energy Commission Report LAMS-2379 (Los Alamos Scientific Laboratory, Los Alamos, N.M.). 1960.

48. Lottes, P.A. Experimental studies of natural circulation boiling and their application to boiling reactor performance. Second International Conference on Peaceful Uses of Atomic Energy, Geneva, Switzerland. Paper 1983. United Nations, New York, N.Y. 1958.

49. _____. Reactor heat transfer. Lecture notes on heat extraction from boiling water power reactors. Sec I:5-24. U.S. Atomic Energy Commission Report ANL-6063 (Argonne National Laboratory, Argonne, Illinois). 1959.

50. _____ and Flinn, W.S. A method of analysis of natural circulation boiling systems. Nuclear Science and Engineering 1:461-476. 1956.

51. _____, Petrick, M. and Marchaterre, J.F. Lecture notes on heat extraction from boiling water power reactors. U.S. Atomic Energy Commission Report ANL-6063 (Argonne National Laboratory, Argonne, Illinois). 1959.

52. Martinelli, R.C. and Nelson, D.B. Prediction of pressure drop during forced-circulation boiling of water. American Society of Mechanical Engineers Transactions 78:695-702. 1948.

53. Maurer, G.W. A method of predicting steady-state boiling vapor fractions in reactor coolant channels. U.S. Atomic Energy Commission Report WAPD-BT-19 (Westinghouse Electric Corp. Atomic Power Division, Pittsburgh, Pa.). 1960.

54. Meyer, J.E. Conservation laws in one dimensional hydrodynamics. U.S. Atomic Energy Commission Report WAPD-BT-20 (Westinghouse Electric Corp. Atomic Power Division, Pittsburgh, Pa.). 1960.

55. _____ and Williams, J.S., Jr. A momentum integral model for the treatment of transient fluid flow. U.S. Atomic Energy Commission Report WAPD-BT-25 (Westinghouse Electric Corp. Atomic Power Division, Pittsburgh, Pa.). 1962.

56. Miller, R.I. and Pyle, R.S. IITE--A digital program for the prediction of two-dimensional two-phase hydrodynamics. U.S. Atomic Energy Commission Report WAPD-TM-240 (Westinghouse Electric Corp. Atomic Power Division, Pittsburgh, Pa.). 1962.

57. Noyes, R.C., Bergonzoli, F., and Gingrich, J.E. FUGUE, a non-dimensional method for digital computer calculation of steady state temperature, pressure, and void fraction in pipe flow with or without boiling. U.S. Atomic Energy Commission Report NAA-SR-5958 (North American Aviation, Inc. Downey, California). 1961.

58a. Petrick, M. A study of vapor carryunder and associated problems. U.S. Atomic Energy Commission Report ANL-6581 (Argonne National Laboratory, Argonne, Illinois). 1962.

58b. _____ and Spleha, E.A. Thermal hydraulic performance characteristics of EBWR (0 to 100 Mwt.). U.S. Atomic Energy Commission Report ANL-6693 (Argonne National Laboratory, Argonne, Illinois). 1963.

59. Quandt, E.R. Jr. Analysis of parallel channel transient response and flow oscillations. U.S. Atomic Energy Commission Report WAPD-AD-TH-489 (Westinghouse Electric Corp. Atomic Power Division, Pittsburgh, Pa.). 1959.

60. Quinn, E.P. and Case, J.M. Natural circulation loop performance at 1000 psia under periodic accelerations. U.S. Atomic Energy Commission Report GEAP-3997 Rev. 1 (General Electric Company, Atomic Power Dept., San Jose, California). 1960.

61. Richtmeyer, R.D. Difference methods for initial-value problems. New York, N.Y., Interscience Publishers, Inc. 1957.

62. Schrock, V.E. Transient boiling experiments. Proceedings of the 1960 Idaho conference on reactor kinetics. U.S. Atomic Energy Commission Report IDO-16791 209-230 (Idaho Operations Office, AEC, Idaho Falls, Idaho). 1960.

63. Thie, J.A. Boiling water reactor instability. Nucleonics 16:102-111. March 1958.

64. _____. Dynamic behavior of boiling reactors. U.S. Atomic Energy Commission Report ANL-5849 (Argonne National Laboratory, Argonne, Illinois). 1959.

65. Vennard, J.K. Elementary fluid mechanics. 4th ed. New York, N.Y., John Wiley and Sons, Inc. 1960.

66. Wilson, J.F. Velocity of rising steam in a bubbling two-phase mixture. American Nuclear Society Transactions 5:150-151. 1962.

67. Wissler, E.H. The transient behavior of a two-phase natural convection loop. Unpublished Ph.D. thesis. Minneapolis, Minn., Library, University of Minnesota. 1958. Original not available; cited in Anderson, R.P., and Lottes, P.A. Boiling stability. Progress in Nuclear Energy, Ser. IV, Vol. 4:11-16. New York, N.Y., Pergamon Press. 1961.

68. _____, Isben, H.S. and Amundson, N.R. The oscillatory behavior of a two-phase natural circulation loop. American Institute of Chemical Engineers Journal 2:157-162. 1956.

69. Wright, R.M. Flow in down-flow forced convection boiling tubes. U.S. Atomic Energy Commission Report UCRL-9744 (California. University, Berkley. Radiation Laboratory). 1961.

70. Zivi, S.M. Kinetic studies of hetrogeneous water reactors. U.S. Atomic Energy Commission Report TID-16589 (Technical Information Service Extension, AEC). 1962.

71. _____. Measurement and interpretation of transfer functions of hydrodynamic instabilities in boiling loop experiments. Advanced course on the dynamic behavior of boiling water reactors, Kjeller, Norway, 1962. U.S. Atomic Energy Commission Report KR-35, Vol. 2 I.1-I.45. (Norway Institutt for Atomenergi, Kjeller). 1963.

72. Zuber, N. Nucleate boiling, the region of isolated bubbles and the similarity with natural convection. International Journal of Heat and Mass Transfer 6:53.78. January 1963.

73. _____. Thermal hydraulic instability. Proceedings of the 1960 Idaho conference on reactor kinetics. U.S. Atomic Energy Commission Report IDO-16791 189-209 (Idaho Operations Office, AEC, Idaho Falls, Idaho). 1960.